

000 001 002 003 004 005 006 007 008 009 010 011 012 DRAW-IN-MIND: REBALANCING DESIGNER-PAINTER 001 ROLES IN UNIFIED MULTIMODAL MODELS BENEFITS 002 IMAGE EDITING

006 **Anonymous authors**

007 Paper under double-blind review

011 ABSTRACT

013 In recent years, integrating multimodal understanding and generation into a sin-
014 gle unified model has emerged as a promising paradigm. While this approach
015 achieves strong results in text-to-image (T2I) generation, it still struggles with
016 precise image editing. We attribute this limitation to an imbalanced division of
017 responsibilities. The understanding module primarily functions as a translator
018 that encodes user instructions into semantic conditions, while the generation mod-
019 ule must simultaneously act as designer and painter, inferring the original layout,
020 identifying the target editing region, and rendering the new content. This imbal-
021 ance is counterintuitive because the understanding module is typically trained with
022 several times more data on complex reasoning tasks than the generation module.
023 To address this issue, we introduce *Draw-In-Mind* (DIM), a dataset comprising
024 two complementary subsets: **(i)** DIM-T2I, containing 14M long-context image-
025 text pairs to enhance complex instruction comprehension; and **(ii)** DIM-Edit, con-
026 sisting of 233K chain-of-thought imaginations generated by GPT-4o, serving as
027 explicit design blueprints for image edits. We connect a frozen Qwen2.5-VL-
028 3B (Bai et al., 2025) with a trainable SANA1.5-1.6B (Xie et al., 2025a) via a
029 lightweight two-layer MLP, and train it on the proposed DIM dataset, resulting in
030 DIM-4.6B-T2I/Edit. Despite its modest parameter scale, DIM-4.6B-Edit achieves
031 SOTA or competitive performance on the ImgEdit and GEdit-Bench benchmarks,
032 outperforming much larger models such as UniWorld-V1 (Lin et al., 2025) and
033 Step1X-Edit (Liu et al., 2025). These findings demonstrate that explicitly as-
034 signing the design responsibility to the understanding module provides significant
035 benefits for image editing. Our dataset and models will be publicly available.

036 1 INTRODUCTION

038 Over the past few years, considerable effort has been devoted to developing unified models cap-
039 able of both multimodal understanding and generation. Many such trials, *e.g.*, Show-o (Xie et al.,
040 2024) and MetaQuery (Pan et al., 2025), have achieved impressive results on T2I generation, yet
041 this paradigm falters when extended to instruction-guided image editing. Even recent methods such
042 as BAGEL (Deng et al., 2025), UniWorld-V1 (Lin et al., 2025), and Step1X-Edit (Liu et al., 2025)
043 struggle, as evidenced by the substantial performance gap with proprietary models like GPT-4o-
044 Image (OpenAI, 2025) on the ImgEdit and GEdit-Bench benchmarks. While much concurrent re-
045 search focuses on scaling parameters and data or on architectural modifications, in this paper we
046 identify a novel challenge underlying current image editing models: *a fundamental imbalance divi-*
047 *sion of responsibilities between the understanding and generation modules.*

048 Specifically, we observe that current image editing models often translate user instructions into
049 semantic conditions through a semantic encoder, typically a multimodal large language model, yet
050 this process lacks intermediate reasoning or refinement. The resulting conditions are then forwarded
051 to the generation module, which is responsible for completing the editing process. At this stage, the
052 generation module must simultaneously infer the original layout, determine the editing region, and
053 render the new content. In this paradigm, the understanding module functions merely as a translator,
while the generation module is burdened with the demanding tasks of both design and painting.

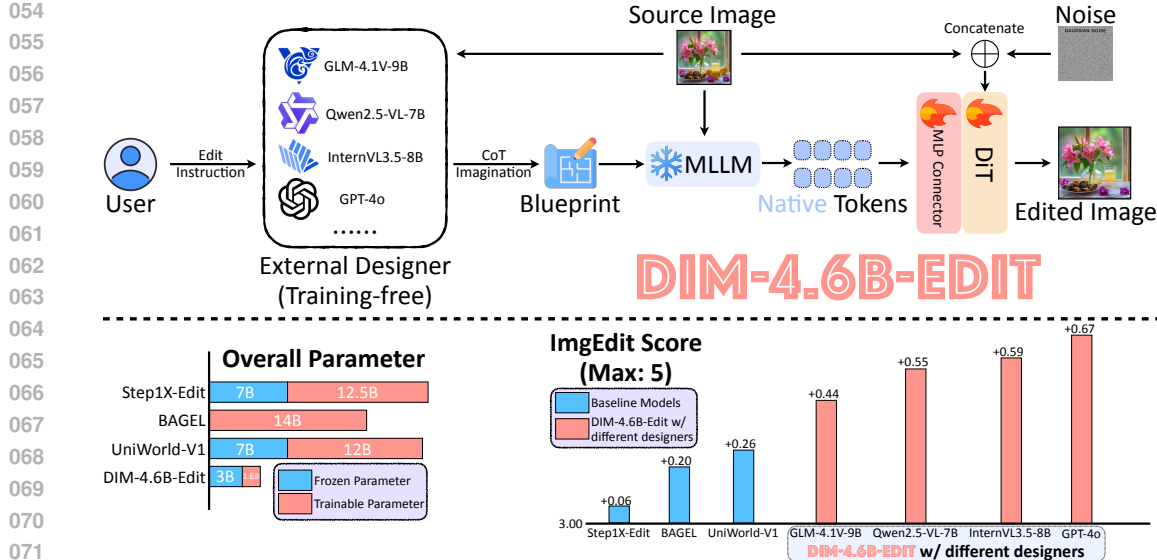


Figure 1: **Upper:** We employ a lightweight MLP connector to bridge a frozen MLLM, *i.e.*, Qwen2.5-VL-3B (Bai et al., 2025), with a trainable DiT, *i.e.*, SANA1.5-1.6B (Xie et al., 2025a), forming DIM-4.6B-Edit. In the editing process, we first leverage an external designer to produce a textual blueprint in a chain-of-thought style, which is then provided to DIM-4.6B-Edit to carry out precise image editing. **Lower:** DIM-4.6B-Edit establishes new state-of-the-art results on the challenging ImgEdit benchmark across diverse designers, while requiring 5× fewer parameters than existing frontier models. These results highlight both the effectiveness of the proposed DIM dataset and the generalizability of our approach.

This arrangement contrasts with natural human workflows, where planning and refinement typically precede the act of drawing. A more intuitive strategy is therefore to assign design-oriented reasoning to the understanding module while allowing the generation module to focus exclusively on painting.

Motivated by this observation, we introduce *Draw-In-Mind* (DIM), a dataset consisting of two complementary subsets: (i) DIM-T2I that contains 14M long-context image-text pairs annotated across 21 dimensions by in-house models to lay the groundwork for complex chain-of-thought comprehension; and (ii) DIM-Edit that comprises 233K high-quality chain-of-thought imagination generated by GPT-4o from existing image editing data, enabling the model to interpret explicit design plans from an external designer. We then establish a simple baseline by concatenating a frozen MLLM, *i.e.*, Qwen2.5-VL-3B, with a trainable DiT, *i.e.*, SANA1.5-1.6B, via a two-layer MLP and train it end-to-end on both public data and the proposed DIM dataset, resulting in DIM-4.6B-T2I/Edit. During edit inference, we employ an arbitrary external designer, feeding its chain-of-thought imagination into the model to guide precise image edits. The framework and performance overview are illustrated in Figure 1. Despite its simplicity, DIM-4.6B-Edit matches or outperforms 5× larger models such as Step1X-Edit (Liu et al., 2025) and UniWorld-V1 (Lin et al., 2025) on the ImgEdit benchmark. These results validate the effectiveness of the proposed DIM dataset and confirm the benefit of shifting the design responsibility from the generation module to the understanding module.

To summarize, we make the following contributions in this paper:

- We pinpoint a fundamental imbalanced division of responsibilities in current image editing models, which overburdens the generation module with both design and painting tasks.
- We introduce *Draw-In-Mind* (DIM), a unified dataset with two complementary subsets: DIM-T2I and DIM-Edit. This dataset explicitly frees the generation module from design responsibility and enables it to concentrate on painting, leading to substantial improvements in editing performance.
- We establish a simple baseline by connecting a frozen Qwen2.5-VL-3B with a trainable SANA1.5-1.6B via a two-layer MLP and train it on DIM. Despite its modest size and simple architecture, DIM-4.6B-Edit outperforms 5× larger competitors, validating the efficacy of DIM.

108

2 RELATED WORK

109

2.1 EXISTING IMAGE GENERATION DATASETS

110 **T2I Datasets.** Existing T2I datasets have provided many high-quality image-text pairs. They can be
 111 roughly grouped into three categories: (i) *purely AI-generated* data, *e.g.*, JourneyDB (Sun et al.,
 112 2023) and MidJourney-V6 (CortexLM, 2025), which collect images from the MidJourney API,
 113 and HQ-Edit (Hui et al., 2024), which generates images via DALL-E 3; (ii) *real-world* data, *e.g.*,
 114 COCO (Lin et al., 2014), which harvests images from Flickr and annotates them by human workers;
 115 and (iii) *mixed* data, *e.g.*, InstructP2P (Brooks et al., 2023), which sources real images from LAION-
 116 Aesthetics and produces edited variants via Prompt2Prompt (Hertz et al., 2022). Although these
 117 datasets deliver high perceptual quality, their prompts are typically short, limiting their utility for
 118 complex chain-of-thought reasoning in the editing stage. To ensure broad concept coverage, we opt
 119 for harvesting real-world images and annotate them with our in-house models from 21 dimensions,
 120 yielding 14M long-context image-text pairs, namely DIM-T2I, that form a robust foundation for
 121 complex CoT-guided editing.

122 **Image Editing Datasets.** Most large-scale image editing datasets either employ AI editors for end-
 123 to-end modification, *e.g.*, InstructP2P (Brooks et al., 2023) and HQ-Edit (Hui et al., 2024), or adopt
 124 a two-stage pipeline that first localizes the edit region via grounding models and then applies in-
 125 painting to alter the target objects, *e.g.*, UltraEdit (Zhao et al., 2024). A few efforts enlist human
 126 experts to annotate small-scale but high-quality edit pairs, *e.g.*, MagicBrush (Zhang et al., 2023) and
 127 SEED-Data-Edit-Part3 (Ge et al., 2024). However, their instructions are typically brief and occa-
 128 sionally misaligned with the corresponding image pairs. In contrast, our DIM-Edit comprises 233K
 129 deliberately designed chain-of-thought imaginations derived from these existing editing datasets.
 130 These rich and detailed CoT instructions act as explicit design blueprints, lighten the cognitive load
 131 on the generation module, and significantly improve editing performance.

132

2.2 UNIFIED MODELS FOR IMAGE GENERATION

133 **T2I Models.** In recent years, numerous successful attempts have been made to integrate understand-
 134 ing and generation modules into a unified architecture. These approaches can be broadly categorized
 135 into two technical routes: (i) *Integrative* approaches, *e.g.*, Show-o (Xie et al., 2024) and Janus (Wu
 136 et al., 2025a), which typically adopt an autoregressive generation paradigm to produce both image
 137 and text tokens; and (ii) *Connector-based* approaches, *e.g.*, MetaQuery (Pan et al., 2025), which use
 138 a connector to bridge an understanding module and a generation module. Since the understanding
 139 and generative capabilities are tightly coupled in the former architecture and sometimes lead to con-
 140 flicts that degrade both, we adopt the connector-based design to preserve state-of-the-art cognitive
 141 ability by freezing the understanding module while enhancing generation performance.

142 **Image Editing Models.** When it comes to image editing, the challenge becomes significantly
 143 harder, as neither the latest integrative models (Lin et al., 2025) nor connector-based ones (Liu et al.,
 144 2025) achieve satisfactory performance on mainstream benchmarks such as ImgEdit and GEdit-
 145 Bench compared to proprietary models like GPT-4o-Image, even when employing large-scale under-
 146 standing and generation models such as Qwen2.5-VL-7B (Bai et al., 2025) and FLUX.1-dev (Labs,
 147 2024a). This suggests that simply scaling model size is not an effective strategy for improving im-
 148 age editing capability. In this work, we take a different approach by addressing the problem from
 149 a perspective of *imbalanced division of responsibilities*. We propose DIM-4.6B-Edit, which lever-
 150 ages an external designer to create blueprints in a CoT manner in the textual space before editing.
 151 Despite having only 1.6B generative parameters, our model achieves SOTA editing performance,
 152 highlighting the effectiveness of shifting the design responsibility to the understanding module.

153

3 METHODOLOGY

154

3.1 THE DRAW-IN-MIND (DIM) DATASET

155

3.1.1 DIM-T2I

156 There are typically two strategies to train an editing model, *i.e.*, (i) learning drawing first (T2I), fol-
 157 lowed by adaptation for editing, and (ii) directly learning editing. We observe that the vast majority
 158 of image editing models are built upon established T2I foundations (Brooks et al., 2023; Zhao et al.,
 159 2024; Liu et al., 2025). This aligns with the first strategy and represents a robust technical route

162 that benefits from curriculum learning. Consequently, we elected to achieve basic T2I ability and
 163 subsequently fine-tune the base model for the more challenging editing task.

164 However, we observed that despite the current T2I datasets performing well in terms of prompt-
 165 image alignment and image perceptual quality, the prompts in existing datasets are typically short
 166 and simple, as shown in Table 1. While these prompts accurately capture the semantics of the target
 167 image, they fall short in fostering long-context comprehension, which is an essential foundation for
 168 complex CoT-guided image editing. To bridge this gap, we collect 14M images with resolutions
 169 higher than 512×512 from the web. We believe that the aspects emphasized in widely recognized
 170 understanding datasets and benchmarks effectively capture the most frequent interactions between
 171 humans and objects in the real world. Therefore, we conduct a thorough literature review and an
 172 empirical analysis of existing understanding datasets and benchmarks, and finally derive 21 diverse
 173 dimensions and use internal models to generate long and detailed annotations, thoroughly covering
 174 all dimensions, resulting in DIM-T2I. As shown in Table 1, its average prompt length is at least
 175 twice that of existing corpora, effectively establishing a strong basis for complex CoT-guided image
 176 editing. The dimension-specific prompts and referred datasets/benchmarks are listed in Appendix E.

177 3.1.2 DIM-EDIT

178 As for image editing, the short-
 179 prompt issue is even more pro-
 180 nounced in current datasets. As
 181 shown in Table 1, prompts in main-
 182 stream datasets are generally overly
 183 simplistic, often consisting of only
 184 a few descriptive words. Such data
 185 is not conducive to effective image
 186 editing learning, as the prompts may
 187 fail to accurately reflect the actual
 188 changes between the source and tar-
 189 get images. This phenomenon can
 190 be attributed to two main reasons:
 191 **(i) Inaccurate AI editing or human**
 192 **misoperation.** We observe that even

SOTA proprietary models like GPT-
 193 4o-Image frequently over-edit images, *e.g.*, removing objects not mentioned in the prompts. Such
 194 cases exist widely in AI-generated datasets like ShareGPT-4o-Image and UltraEdit. While in human-
 195 controlled datasets, operators may misunderstand or misapply the edits, resulting in unaligned data.
 196 **(ii) Ambiguous semantics.** Even if the prompt correctly describes the intended change, overly sim-
 197 ple prompts can still result in multiple equally valid edits. For example, in SEED-Data-Edit-Part3,
 198 a common prompt is “change the background”, yet the definition of “background” varies across im-
 199 ages, while in practice the change almost always occurs in the sky, thereby reducing the effectiveness
 200 of the resulting edit data.

201 In addition, existing models typically use the understanding module merely as a translator, directly
 202 converting natural language instructions into semantic conditions. The generator must then rely
 203 on these conditions to simultaneously organize the layout of the edited image, recognize existing
 204 objects, localize the edit area, render new content, and preserve unchanged regions. In other words,
 205 the generator is forced to act as both designer and painter, which is a challenging and counterintuitive
 206 setup. By contrast, humans naturally prepare a mental blueprint before editing and then simply let
 207 their hands follow it to complete the changes.

208 Motivated by the above issues, we propose DIM-Edit, which first optimizes prompts and then imi-
 209 tates human thinking to complete the edits. The DIM-Edit creation pipeline is illustrated in Figure 2.
 210 We construct it from 233K high-quality image pairs collected from three sources: **(i)** 160K highly
 211 consistent edit pairs from UltraEdit, referred to as UltraEdit-160K-CoT, selected using a joint SSIM,
 212 DINOv2 similarity, and CLIP similarity-based filtering; **(ii)** 46K semantically rich samples from the
 213 editing subset of ShareGPT-4o-Image, referred to as ShareGPT-4o-Image-CoT; and **(iii)** 8K human-
 214 edited images from the MagicBrush training set and 19K human-edited images from SEED-Data-
 215 Edit-Part3, specifically targeting remove operations, referred to as HumanEdit-CoT. A detailed data
 collection pipeline can be found in Appendix C.

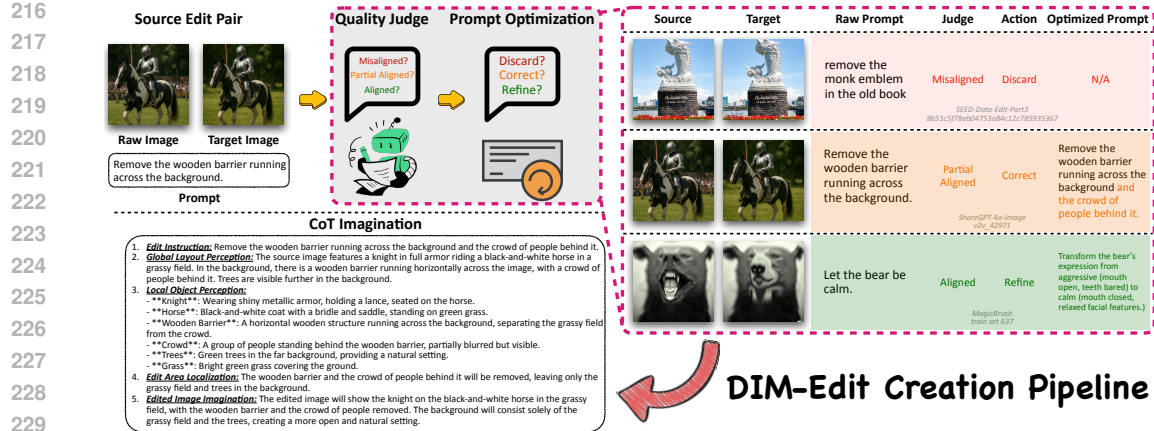


Figure 2: The creation pipeline of DIM-Edit begins with a quality assessment of existing image editing data, followed by prompt optimization using GPT-4o. Finally, the optimized prompts together with the corresponding image pairs are fed into GPT-4o, which generates a four-step chain-of-thought imagination in the textual space.

After collecting raw data, we first sent the raw edit pairs to GPT-4o for prompt quality evaluation, as shown in Figure 2. The results are categorized into three groups: (i) *Misaligned*. The prompt does not reflect the actual edit at all, possibly due to misannotation or misoperation. (ii) *Partially aligned*. The target image exhibits over-editing, *i.e.*, redundant objects are added to or removed from the source image. (iii) *Aligned*. The prompt fully corresponds to the edits.

Next, we take different actions to optimize the prompts based on the judgment: (i) For misaligned prompts, they are discarded outright. (ii) For partially aligned prompts, we ask GPT-4o to add details about unmentioned changes, *e.g.*, including objects that were incorrectly removed in the prompt. (iii) For aligned prompts, we instruct GPT-4o to remove ambiguity and refine the prompt, for example, by specifying the exact objects to be edited to avoid confusion with visually similar objects.

Finally, we provide the optimized prompts, along with the source image to GPT-4o and instruct it to produce a four-step CoT imagination that emulates human editing behavior. For the sake of accuracy, we also provide the target image to it for reference. The target of each CoT step is as follows: (i) *Global Layout Perception*: identify and describe all key objects and their positions in the source image. (ii) *Local Object Perception*: describe the appearance of each object or background element in the source image, including shape, color, texture, and state. (iii) *Edit Area Localization*: specify which objects or regions will be modified, based on the refined instruction. (iv) *Edited Image Imagination*: describe the expected appearance of the edited image, with an emphasis on the modified areas. As shown in Table 1 and Figure 2, the resulting CoT imagination is not only ultra-long but also highly accurate, effectively removing the design responsibility from the generation module and thereby significantly enhancing the efficiency of image editing learning. **A quality assessment of the CoTs involving both MLLMs and human verification can be found in Appendix D.**

3.2 DIM-4.6B-T2I/EDIT

Leveraging MLLMs to provide multimodal conditions for image generation has become a common practice recently. In this work, we first build a base T2I model and then adapt it to the editing task.

For the base T2I model, we start by establishing a simple baseline, similar to MetaQuery (Pan et al., 2025), to preserve state-of-the-art understanding capability. We select Qwen2.5-VL-3B (Bai et al., 2025) as the MLLM and SANA1.5-1.6B (Xie et al., 2025a) as the diffusion decoder for their modest size. Unlike MetaQuery, which employs a large 24-layer transformer with 1.6B parameters as a connector between the MLLM and the diffusion decoder, we adopt a much simpler design, *i.e.*, a two-layer MLP, to directly project multimodal tokens into the generation space. We refer to this model as DIM-4.6B-T2I, illustrated in Figure 1. We train DIM-4.6B-T2I on a mixture of the proposed DIM-T2I dataset and an additional 6.9M image-text pairs from MidJourney-V6 (CortexLM, 2025), COCO (Lin et al., 2014), InstructP2P (Brooks et al., 2023), JourneyDB (Sun et al., 2023), HQ-Edit (Hui et al., 2024), and Dimba (Fei et al., 2024). During training, Qwen2.5-VL-3B remains

270
 271 Table 2: The text-to-image generation performance on **GenEval** and **MJHQ-30K**. \uparrow and \downarrow indicate
 272 that higher and lower values are better, respectively; \dagger denotes using an LLM rewriter;  and  denote frozen and trainable parameters, respectively.
 273

274 275 Model	276 Params	277 GenEval \uparrow						278 MJHQ-30K \downarrow	
		279 Single Obj.	280 Two Obj.	281 Counting	282 Colors	283 Position	284 Attr.	285 Overall	286 FID
<i>Gen. Only</i>									
PixArt- α (Chen et al., 2023)	0.6B 	0.98	0.50	0.44	0.80	0.08	0.07	0.48	6.14
SDXL (Podell et al., 2023)	2.6B 	0.98	0.74	0.39	0.85	0.15	0.23	0.55	8.76
DALL-E-3 (Betker et al., 2023)	-	0.96	0.87	0.47	0.83	0.43	0.45	0.67	-
SD3-Medium (Esser et al., 2024)	2.0B 	0.99	0.94	0.72	0.89	0.33	0.60	0.74	11.92
<i>Unified</i>									
Janus (Wu et al., 2025a)	1.3B 	0.97	0.68	0.30	0.84	0.46	0.42	0.61	10.10
Emu3-Gen \dagger (Wang et al., 2024b)	8.0B 	0.99	0.81	0.42	0.80	0.49	0.45	0.66	-
Show-o (Xie et al., 2024)	1.3B 	0.98	0.80	0.66	0.84	0.31	0.50	0.68	15.18
Show-o2-7B (Xie et al., 2025b)	7.0B 	1.00	0.87	0.58	0.92	0.52	0.62	0.76	-
Janus-Pro-7B (Chen et al., 2025c)	7.0B 	0.99	0.89	0.59	0.90	0.79	0.66	0.80	13.48
BAGEL (Deng et al., 2025)	14.0B 	0.99	0.94	0.81	0.88	0.64	0.63	0.82	-
MetaQuery-L \dagger (Pan et al., 2025)	3.0B  3.2B 	-	-	-	-	-	-	0.78	6.35
DIM-4.6B-T2I \dagger	3.0B  1.6B 	0.99	0.89	0.63	0.86	0.62	0.61	0.77	5.50

287 frozen, and we finetune only the parameters of the connector and SANA1.5-1.6B. Notably, distillation
 288 datasets like BLIP3-o-60K (Chen et al., 2025a) explicitly curate data to align with the structural
 289 patterns of benchmarks like GenEval, we exclude them to avoid any risk of data leakage (Wu et al.,
 290 2025b) or benchmark hacking in the evaluation to justify the contribution of our DIM data. We
 291 adopt vanilla flow matching as the sole objective, avoiding parameter-tuning tricks to highlight data
 292 effectiveness and maintain simplicity.

293
 294 Thanks to the rich world knowledge and high-quality long-context prompts in DIM-T2I, the trained
 295 DIM-4.6B-T2I model provides a strong foundation for complex CoT comprehension. We then adopt
 296 a two-stage training strategy to adapt it for the editing task. In the first stage, we initialize the editing
 297 model from DIM-4.6B-T2I and fine-tune it on the UltraEdit (Zhao et al., 2024) dataset to develop
 298 basic editing capability. Following InstructP2P (Brooks et al., 2023), we concatenate the source
 299 image with noise along the channel dimension, as illustrated in Figure 1. In the second stage, we
 300 fine-tune the stage-one model exclusively on the proposed DIM-Edit dataset, resulting in DIM-4.6B-
 301 Edit. During inference, we employ an external designer to prepare a blueprint in the same format as
 302 DIM-Edit, except without access to the target image, ensuring alignment with real usage scenarios.

303 4 EXPERIMENTS

304 4.1 EXPERIMENTAL SETUP

305 During training, we use AdamW as the optimizer and keep most hyperparameters unchanged for
 306 simplicity. For DIM-4.6B-T2I, we first warm up by training only the connector for one epoch with a
 307 learning rate of 2×10^{-5} , then jointly train the connector and SANA1.5-1.6B for eight epochs with
 308 the same rate and a batch size of 256. For DIM-4.6B-Edit, we set the batch size to 32, training on
 309 UltraEdit for 10 epochs at a 1×10^{-4} learning rate, then finetuning on DIM-Edit for 50 epochs at a
 310 1×10^{-5} learning rate. During inference, GPT-4o serves as the designer unless otherwise specified.

311 Although the primary focus of this paper is image editing, we evaluate DIM-4.6B-T2I on T2I benchmarks
 312 to verify the effectiveness of DIM-T2I. We report the GenEval (Ghosh et al., 2023) scores
 313 and MJHQ-30K (Li et al., 2024b) FID. Following MetaQuery (Pan et al., 2025) and Emu3 (Pan
 314 et al., 2025), we test LLM-rewritten prompts for GenEval evaluation. For image editing, we report
 315 scores on the recently proposed ImgEdit (Lin et al., 2025) and GEdit-Bench-EN (Liu et al., 2025)
 316 benchmarks, using GPT-4.1 for evaluation to ensure fair comparison with existing results. We also
 317 report results on MagicBrush (Zhang et al., 2023) to show the performance on automated metrics.

318 4.2 MAIN RESULTS

319 4.2.1 TEXT-TO-IMAGE GENERATION

320 We first report T2I performance on GenEval and MJHQ-30K in Table 2. Our DIM-4.6B-T2I adopts
 321 a simple architecture with very few trainable parameters yet achieves SOTA or competitive per-
 322 formance, demonstrating the high data quality of DIM-T2I. For semantic alignment, DIM-4.6B-

324
 325 Table 3: The image editing performance on **ImgEdit**. We use GPT-4.1 for evaluation to ensure
 326 consistency with the existing results reported in UniWorld-V1. * indicates results evaluated by us
 327 using the official weights; and denote frozen and trainable parameters, respectively.

328 Model	329 Params	330 Add	331 Adjust	332 Extract	333 Replace	334 Remove	335 Background	336 Style	337 Hybrid	338 Action	339 Overall
MagicBrush (Zhang et al., 2023)	0.9B	2.84	1.58	1.51	1.97	1.58	1.75	2.38	1.62	1.22	1.83
Instruct-P2P (Brooks et al., 2023)	0.9B	2.45	1.83	1.44	2.01	1.50	1.44	3.55	1.20	1.46	1.88
AnyEdit (Yu et al., 2025)	1.3B	3.18	2.95	1.88	2.47	2.23	2.24	2.85	1.56	2.65	2.45
UltraEdit (Zhao et al., 2024)	2.0B	3.44	2.81	2.13	2.96	1.45	2.83	3.76	1.91	2.98	2.70
Step1X-Edit (Liu et al., 2025)	7.0B 12.5B	3.88	3.14	1.76	3.40	2.41	3.16	4.63	2.64	2.52	3.06
BAGEL (Deng et al., 2025)	14.0B	3.56	3.31	1.70	3.30	2.62	3.24	4.49	2.38	4.17	3.20
UniWorld-V1 (Lin et al., 2025)	7.0B 12.0B	3.82	3.64	2.27	3.47	3.24	2.99	4.21	2.96	2.74	3.26
Janus-4o* (Chen et al., 2025b)	7.0B	3.35	3.35	2.25	3.01	2.18	3.32	4.71	2.49	4.04	3.19
GPT-4o-Image (OpenAI, 2025)	-	4.61	4.33	2.90	4.35	3.66	4.57	4.93	3.96	4.89	4.20
DIM-4.6B-Edit	3.0B 1.6B	4.09	3.47	2.30	4.00	3.43	3.87	4.92	2.85	4.08	3.67

338 Table 4: The overall task-wise performance on **GEdit-Bench-EN** Full set. * indicates results evaluated
 339 by us. Task abbreviations: Background Change (BC), Color Alter (CA), Material Alter (MA),
 340 Motion Change (MC), PS Human (PH), Style Change (SC), Subject-Add (SA), Subject-Remove
 341 (SRM), Subject-Replace (SRP), Text Change (TC), Tone Transfer (TT), and Average (AVG).

342 Model	343 BC	344 CA	345 MA	346 MC	347 PH	348 SC	349 SA	350 SRM	351 SRP	352 TC	353 TT	354 AVG	355 AVG w/o TC
UniWorld-V1 (Lin et al., 2025)	4.92	6.37	4.79	1.85	4.03	5.64	7.23	6.17	5.70	1.15	5.54	4.85	5.22
Janus-4o* (Chen et al., 2025b)	4.31	5.02	4.41	2.71	4.09	5.80	4.07	1.69	3.69	2.35	3.96	3.83	3.97
Step1X-Edit (Liu et al., 2025)	7.03	6.26	6.46	3.66	5.23	7.24	7.17	6.42	7.39	7.40	6.62	6.44	6.35
DIM-4.6B-Edit	7.02	6.81	6.00	4.67	5.88	7.16	7.48	6.67	6.76	2.99	6.55	6.18	6.50

346 T2I shows only a small gap compared to much larger models like BAGEL (Deng et al., 2025) on
 347 GenEval. Compared with MetaQuery (Pan et al., 2025), which employs a large 1.6B-parameter connector
 348 for query learning, our model achieves nearly the same performance using only a two-layer
 349 MLP connector and naive multimodal tokens. In addition, it attains optimal perceptual quality, as
 350 evidenced by the lowest FID on the aesthetics-oriented MJHQ-30K benchmark. These results indicate
 351 that *even without complex aesthetic filtering, carefully crafted long-context prompts enable*
 352 *robust text-to-image generation*, offering a practical approach for rapid large-scale dataset creation
 353 by directly harvesting images from the web.

354 4.2.2 IMAGE EDITING

355 The image editing performance on ImgEdit is reported in Table 3. Our DIM-4.6B-Edit shows a
 356 significant improvement over previously available open source models. In comparison with other
 357 connector-based architectures such as Step1X-Edit and UniWorld-V1, which rely on a 12B FLUX
 358 backend for generation together with a 7B multimodal large language model for condition translation,
 359 DIM-4.6B-Edit achieves superior results while maintaining both a much smaller total parameter
 360 count and a very limited number of trainable parameters.

361 Since DIM-Edit includes high-quality images from ShareGPT-4o-Image (Chen et al., 2025b), we
 362 also evaluate Janus-4o, which is trained on the same dataset, for reference. Janus-4o achieves only
 363 suboptimal results, indicating that the improvement comes from DIM-Edit itself, whose natural and
 364 precise edit blueprints substantially enhance editing performance. These encouraging results validate
 365 our assumption that imbalanced division of responsibilities degrades image editing, confirm
 366 the soundness of our data creation pipeline, and highlight the effectiveness of the Draw-In-Mind
 367 paradigm: assigning the design responsibility to the understanding module while allowing the
 368 generation module to focus on actual editing exclusively.

369 We further demonstrate the capability of DIM-4.6B-Edit through intuitive visual comparisons of
 370 editing results on four AI-generated out-of-domain images in Figure 3. Janus-4o exhibits severe
 371 distortions despite being trained on GPT-4o-generated edit pairs, while Step1X-Edit produces less
 372 natural edits (rows 2-4) and fails in complex scenarios such as row 1, which involves manipulating
 373 multiple objects. In contrast, DIM-4.6B-Edit successfully follows the instructions to produce natural
 374 and consistent edited images. Please refer to Appendix A for more visualizations.

375 We also include overall task-wise performance on GEdit-Bench-EN in Table 4. The results reveal a
 376 similar pattern as reported in UniWorld-V1 (Lin et al., 2025): Step1X-Edit achieves notable gains
 377 in the Text Change task, whereas other models, including ours, perform less effectively due to the



Figure 3: **Green** and **Blue** : the edits of Janus-4o and Step1X-Edit; **Red** : the edits of our models trained on different data corpora. All variants are tuned from the base checkpoint \bowtie in Table 8.

Table 5: **The MagicBrush** test set performance. Metrics are calculated between human-edited groundtruth and AI-generated edits. and denote the 1st and 2nd best model, respectively.

Method	Gen Params	L1 \downarrow	CLIP-I \uparrow	DINO \uparrow
InstructP2P (Brooks et al., 2023)	0.9B	0.114	0.851	0.744
MagicBrus (Zhang et al., 2023)	0.9B	0.074	0.908	0.847
UltraEdit (Zhao et al., 2024)	2.0B	0.066	0.904	0.852
FluxEdit (Paul, 2025)	12.0B	0.114	0.779	0.663
FLUX.1 Fill (Labs, 2024b)	12.0B	0.192	0.795	0.669
RF-Solver Edit (Wang et al., 2024a)	12.0B	0.112	0.766	0.675
ACE++ (Mao et al., 2025)	12.0B	0.195	0.741	0.591
ICEedit (Zhang et al., 2025)	12.0B	0.060	0.928	0.853
DIM-4.6B-Edit	1.6B	0.065	0.928	0.882

absence of such data in DIM-Edit. Excluding the Text Change task, DIM-4.6B-Edit beats Step1X-Edit while maintaining a compact size, underscoring the high efficacy of our CoT data. Please refer to Appendix A for full GEdit-Bench-EN results.

We further conduct evaluation on the MagicBrush to test automated pixel-to-pixel metrics computed between human-edits and AI-edits. The results are presented in Table 5. DIM-4.6B-Edit achieves SOTA performance. Notably, ICEedit employs a 12B FLUX.1 Fill backbone, with MagicBrush samples constituting approximately 20% of its total training set. In contrast, DIM-4.6B-Edit utilizes a compact 1.6B generation backbone, where MagicBrush data accounts for less than 3% of our DIM-Edit dataset. These comparable results validate the effectiveness of the Draw-In-Mind paradigm and the generalizability of our DIM-Edit CoT. Despite our training distribution being significantly less driven by MagicBrush data, our model matches the performance of 5 \times larger competitors.

4.3 ABLATION STUDY

Generalizability to External Designers. Although our proposed DIM-Edit is annotated with GPT-4o, we show that the resulting DIM-4.6B-Edit is compatible with various external designers, as reported in Table 6. In the first row, we remove the designer and directly use the raw prompt from ImgEdit. Even under this setting, DIM-4.6B-Edit achieves performance comparable to frontier models such as BAGEL, demonstrating that high-quality CoT annotations help strengthen basic editing by mitigating prompt–edit misalignment. We then replace GPT-4o with four mainstream MLLMs as external designers, *i.e.*, Qwen2.5-VL-7B (Bai et al., 2025), MiMo-VL-7B (Xiaomi,

432

433

Table 6: The **ImgEdit** performance *w.r.t.* different *external* designers.

External Designer	Add	Adjust	Extract	Replace	Remove	Background	Style	Hybrid	Action	Overall
-	3.53	3.23	2.01	3.49	1.47	3.42	4.79	2.35	3.64	3.10
Qwen2.5-VL-7B (Bai et al., 2025)	3.95	3.35	2.25	3.85	3.31	3.57	4.88	2.81	4.02	3.55
MiMo-VL-7B (Xiaomi, 2025)	3.95	3.32	2.20	3.75	2.46	3.82	4.88	2.52	3.93	3.43
InternVL3.5-8B (Wang et al., 2025)	3.98	3.40	2.05	4.14	3.30	3.84	4.94	2.77	3.89	3.59
GLM-4.1V-9B (Hong et al., 2025)	3.95	3.27	2.23	3.90	2.64	3.81	4.92	2.23	4.02	3.44
GPT-4o (Hurst et al., 2024)	4.09	3.47	2.30	4.00	3.43	3.87	4.92	2.85	4.08	3.67

434

435

436

437

438

439

440

441

Table 7: The **ImgEdit** performance *w.r.t.* the *internal* Qwen2.5-VL-3B designer.

Internal Designer	Add	Adjust	Extract	Replace	Remove	Background	Style	Hybrid	Action	Overall
-	3.53	3.23	2.01	3.49	1.47	3.42	4.79	2.35	3.64	3.10
Qwen2.5-VL-3B 	3.80	3.24	2.03	3.89	3.21	3.52	4.92	2.71	4.05	3.49
Qwen2.5-VL-3B 	3.96	3.36	2.25	3.98	3.31	3.81	4.95	2.83	4.02	3.61
GPT-4o	4.09	3.47	2.30	4.00	3.43	3.87	4.92	2.85	4.08	3.67

442

443

444

445

446

447

448

449

450

451

452

453

2025), InternVL3.5-8B (Bai et al., 2025), and GLM-4.1V-9B (Hong et al., 2025). All of them deliver strong results compared to previous state-of-the-art models in Table 3, highlighting the robustness of DIM-4.6B-Edit and the generalizability of our DIM framework. Furthermore, models equipped with external designers significantly outperform the raw-prompt setting, confirming that CoT imagination effectively reduces the burden on the generation modules and enhances overall editing quality.

454

455

456

457

458

459

460

461

462

463

Integrated End-to-End Evaluation. To exclude potential influence from external designers, we establish a “self-play” configuration. In this setup, CoT embeddings generated by the internal MLLM (Qwen2.5-VL-3B) are directly fed into the painter to execute edits, effectively eliminating the need for the external inference round. The result (Table 7 2nd row) shows that this “self-play” model achieves SOTA performance, validating the effectiveness of the Draw-In-Mind paradigm and the high quality of the DIM-Edit data. We further investigate whether the CoT blueprints in DIM-Edit can serve as a corpus to bridge the gap between open-source and closed-source designers. To this end, we perform lightweight fine-tuning on Qwen2.5-VL-3B and subsequently feed its blueprints into DIM-4.6B-Edit. The results (Table 7 3rd row) demonstrate that fine-tuning from DIM-Edit’s CoTs can effectively mitigate the performance disparity with the proprietary models like GPT-4o.

464

465

466

467

468

469

470

471

472

473

474

475

476

477

478

479

Data Composition. In Table 8, we present a rigorous data composition analysis for the editing task to identify the sources of performance improvements. In the first stage, we observe that training solely on ShareGPT-4o-Image already yields a satisfactory ImgEdit score, indicating strong semantic alignment, which is consistent with the behavior of Janus-4o. However, models trained exclusively on GPT-4o-generated data tend to alter the overall layout noticeably, which is undesirable. In contrast, training on UltraEdit produces slightly lower scores but preserves better consistency between the source and target images. When combining the two datasets, performance improves significantly, as the model benefits from the semantic richness while retaining the edit consistency.

In the second stage, we finetune the checkpoint trained solely on UltraEdit. The effectiveness of our CoT data is demonstrated by comparing row 4 with row 3 in Table 8, where using the CoT version of ShareGPT-4o-Image yields a significant improvement in overall scores compared with its non-CoT counterpart. We also observe that using UltraEdit-160K-CoT alone provides only marginal gains, while the HumanEdit-CoT portion has a more notable impact due to its high edit quality, though still less pronounced than the semantically rich ShareGPT-4o-Image-CoT. When combining all three CoT components, *i.e.*, the proposed DIM-Edit, performance improves substantially once again, indicating that UltraEdit-160K-CoT and HumanEdit-CoT are crucial for maintaining edit consistency, which is consistent with the pattern of row 3.

480

481

482

483

484

485

The visualization of three variants finetuned from the base checkpoint  in Table 8 is shown in Figure 3 for intuitive analysis. The variant tuned on ShareGPT-4o-Image significantly alters the layout despite following the edit prompt, while its counterpart tuned on ShareGPT-4o-Image-CoT preserves more details, indicating that CoT imagination helps maintain editing consistency. However, using ShareGPT-4o-Image-CoT alone still produces unstable edits. In contrast, the model tuned on the full DIM-Edit dataset, *i.e.*, DIM-4.6B-Edit, achieves the best results in both semantic alignment and edit consistency, demonstrating the effectiveness of all three data components in DIM-Edit.

486
 487 Table 8: Impact of data compositions during the two training stages of DIM-4.6B-Edit on **ImgEdit**.
 488 Stage 2 models are tuned from checkpoint .

489 Data Composition	Add	Adjust	Extract	Replace	Remove	Background	Style	Hybrid	Action	Overall
	<i>Stage 1 Non-CoT Data</i>									
491 ShareGPT-4o-Image	3.35	2.74	1.93	3.05	1.95	3.16	4.91	2.00	3.70	2.98
492 UltraEdit-4M 	3.41	3.03	1.91	2.94	1.07	3.09	3.77	2.64	2.97	2.76
493 + ShareGPT-4o-Image	3.85	3.09	1.84	3.71	2.26	3.51	4.88	2.17	3.67	3.22
	<i>Stage 2 CoT Data</i>									
495  + ShareGPT-4o-Image-CoT	4.01	3.19	2.19	3.74	2.53	3.57	4.93	2.25	3.66	3.34
496  + UltraEdit-160K-CoT	3.69	3.21	1.90	2.50	1.22	3.20	3.53	2.71	3.14	2.79
497 + HumanEdit-CoT	3.63	2.99	2.01	3.01	2.64	3.11	3.73	3.03	3.01	3.02
498  + DIM-Edit	4.09	3.47	2.30	4.00	3.43	3.87	4.92	2.85	4.08	3.67

499
 500 Table 9: Impact of CoT compositions on **ImgEdit**. GLP refers to Global Layout Perception, LOP
 501 to Local Object Perception, EAL to Edit Area Localization, and EII to Edited Image Imagination.

502 CoT Composition	Add	Adjust	Extract	Replace	Remove	Background	Style	Hybrid	Action	Overall
503 DIM-Edit	4.09	3.47	2.30	4.00	3.43	3.87	4.92	2.85	4.08	3.67
504 w/o GLP	3.85	3.29	2.06	3.91	3.24	3.55	4.80	2.79	3.92	3.49
505 w/o LOP	3.80	3.15	1.92	3.83	3.07	3.60	4.79	2.44	3.92	3.39
506 w/o EAL	3.79	3.25	1.96	3.73	2.96	3.65	4.81	2.82	3.82	3.42
507 w/o EII	3.77	3.22	1.82	3.88	2.96	3.61	4.78	2.55	3.58	3.35

508 **CoT Composition.** We also analyze the effect of each CoT component by individually removing it,
 509 as shown in Table 8. All components contribute positively to the performance, though their impor-
 510 tance varies. The GLP has only a minor impact, likely because it is an easy task for the generator.
 511 In contrast, the other three CoT components, *i.e.*, LOP, EAL, and EII, have a significant effect. LOP
 512 and EAL require the model to focus on specific regions, while EII demands complex reasoning; none
 513 of these are trivial for the generator. These findings further validate the Draw-In-Mind paradigm,
 514 which reduces the cognitive burden on the generator and thereby improves performance.

515 Table 10: The **ImgEdit** performance of models initialized from scratch/DIM-4.6B-T2I.

516 Initialization	Add	Adjust	Extract	Replace	Remove	Background	Style	Hybrid	Action	Overall
517 Scratch	2.70	2.56	1.93	2.23	2.47	2.82	4.68	2.38	2.15	2.66
518 DIM-4.6B-T2I	4.09	3.47	2.30	4.00	3.43	3.87	4.92	2.85	4.08	3.67

519 **Necessity of DIM-T2I.** Our CoT-guided editing requires robust comprehension capabilities. We
 520 posit that T2I generation is simpler than editing and is better suited for fostering this capability.
 521 Rather than simultaneously tackling two challenging objectives, *i.e.*, complex instruction compre-
 522 hension and image editing, we chose to establish strong instruction comprehension first in the T2I
 523 stage. To justify our assumption, we trained a model exclusively on DIM-Edit to test the feasibility
 524 of simultaneously achieving modality alignment, complex instruction comprehension, and editing
 525 capabilities in a single stage. As evident from the Table 10, the model trained from scratch signifi-
 526 cantly underperforms the version initialized with DIM-4.6B-T2I. This performance gap empirically
 527 validates the necessity of DIM-T2I as a foundational cornerstone for the Draw-In-Mind paradigm.

528 5 CONCLUSION

529 In this paper, we identify a crucial issue in existing image editing models, *i.e.*, *imbalanced division*
 530 of *responsibilities*, where the generator is burdened with complex reasoning, leading to reduced
 531 performance. To address this, we propose the *Draw-In-Mind* (DIM) dataset, consisting of two parts:
 532 **(i)** DIM-T2I, 14M web-crawled image-text pairs with carefully crafted long-context prompts that
 533 provide a foundation for complex CoT comprehension in editing; and **(ii)** DIM-Edit, 233K high-
 534 quality image editing pairs with detailed and precise CoT imagination. By training on the DIM
 535 dataset and incorporating an external designer during editing, we present DIM-4.6B-Edit, which
 536 achieves SOTA or competitive performance on ImgEdit and GEdit-Bench-EN while maintaining a
 537 tiny overall and trainable parameter size. These results validate our motivation to shift the design
 538 responsibility from the generation module to the understanding module, as well as the high efficiency
 539 of our proposed CoT-guided DIM dataset.

540 ETHICS STATEMENT
541

542 All authors of this paper strictly adhere to the ICLR Code of Ethics. The proposed image-text pairs in
543 DIM-T2I have undergone a rigorous safety check to filter harmful content, *e.g.*, NSFW images. The
544 image pairs in DIM-Edit are collected from publicly available datasets, *i.e.*, UltraEdit (Zhao et al.,
545 2024), MagicBrush (Zhang et al., 2023), SEED-Data-Edit-Part3 (Ge et al., 2024), and ShareGPT-
546 4o-Image (Chen et al., 2025b), without introducing new content that may raise ethical concerns.
547 The CoTs generated by GPT-4o were subjected to both OpenAI's internal safety mechanisms and
548 an additional safety check by the authors, confirming that no harmful content is present. Therefore,
549 the training process and the trained models do not introduce ethical issues.

550
551 REPRODUCIBILITY STATEMENT
552

553 The authors take full responsibility for the reproducibility of this work. For the proposed DIM
554 dataset, we provide a detailed data creation pipeline in Section 3.1 and Appendix C, including data
555 sourcing and processing. The prompts used for image annotation are presented in Appendix E.
556 For the DIM-4.6B-T2I/Edit models, we describe their architectures in detail in Section 3.2. In
557 addition, we specify our training configurations and evaluation setup in Section 4.1. We will release
558 the DIM dataset, the DIM-4.6B-T2I/Edit models, and the related code to the public to facilitate
559 reproducibility upon acceptance.

560
561 REFERENCES
562

563 Shuai Bai, Keqin Chen, Xuejing Liu, Jialin Wang, Wenbin Ge, Sibo Song, Kai Dang, Peng Wang,
564 Shijie Wang, Jun Tang, et al. Qwen2. 5-vl technical report. *arXiv preprint arXiv:2502.13923*,
565 2025.

566 James Betker, Gabriel Goh, Li Jing, Tim Brooks, Jianfeng Wang, Linjie Li, Long Ouyang, Juntang
567 Zhuang, Joyce Lee, Yufei Guo, et al. Improving image generation with better captions. *Computer
568 Science*. <https://cdn.openai.com/papers/dall-e-3.pdf>, 2(3):8, 2023.

569 Tim Brooks, Aleksander Holynski, and Alexei A Efros. Instructpix2pix: Learning to follow image
570 editing instructions. In *Proceedings of the IEEE/CVF conference on computer vision and pattern
571 recognition*, pp. 18392–18402, 2023.

572 Jiacheng Chen, Tianhao Liang, Sherman Siu, Zhengqing Wang, Kai Wang, Yubo Wang, Yuansheng
573 Ni, Wang Zhu, Ziyang Jiang, Bohan Lyu, et al. Mega-bench: Scaling multimodal evaluation to
574 over 500 real-world tasks. *arXiv preprint arXiv:2410.10563*, 2024a.

575 Juhai Chen, Zhiyang Xu, Xichen Pan, Yushi Hu, Can Qin, Tom Goldstein, Lifu Huang, Tianyi
576 Zhou, Saining Xie, Silvio Savarese, et al. Blip3-o: A family of fully open unified multimodal
577 models-architecture, training and dataset. *arXiv preprint arXiv:2505.09568*, 2025a.

578 Junsong Chen, Jincheng Yu, Chongjian Ge, Lewei Yao, Enze Xie, Yue Wu, Zhongdao Wang, James
579 Kwok, Ping Luo, Huchuan Lu, et al. Pixart-alpha: Fast training of diffusion transformer for
580 photorealistic text-to-image synthesis. *arXiv preprint arXiv:2310.00426*, 2023.

581 Junying Chen, Zhenyang Cai, Pengcheng Chen, Shunian Chen, Ke Ji, Xidong Wang, Yunjin Yang,
582 and Benyou Wang. Sharegpt-4o-image: Aligning multimodal models with gpt-4o-level image
583 generation. *arXiv preprint arXiv:2506.18095*, 2025b.

584 Lin Chen, Jinsong Li, Xiaoyi Dong, Pan Zhang, Yuhang Zang, Zehui Chen, Haodong Duan, Jiaqi
585 Wang, Yu Qiao, Dahua Lin, et al. Are we on the right way for evaluating large vision-language
586 models? *Advances in Neural Information Processing Systems*, 37:27056–27087, 2024b.

587 Xiaokang Chen, Zhiyu Wu, Xingchao Liu, Zizheng Pan, Wen Liu, Zhenda Xie, Xingkai Yu, and
588 Chong Ruan. Janus-pro: Unified multimodal understanding and generation with data and model
589 scaling. *arXiv preprint arXiv:2501.17811*, 2025c.

594 Karl Cobbe, Vineet Kosaraju, Mohammad Bavarian, Mark Chen, Heewoo Jun, Lukasz Kaiser,
 595 Matthias Plappert, Jerry Tworek, Jacob Hilton, Reiichiro Nakano, et al. Training verifiers to
 596 solve math word problems. *arXiv preprint arXiv:2110.14168*, 2021.

597

598 Gheorghe Comanici, Eric Bieber, Mike Schaeckermann, Ice Pasupat, Noveen Sachdeva, Inderjit
 599 Dhillon, Marcel Blistein, Ori Ram, Dan Zhang, Evan Rosen, et al. Gemini 2.5: Pushing the
 600 frontier with advanced reasoning, multimodality, long context, and next generation agentic capa-
 601 bilities. *arXiv preprint arXiv:2507.06261*, 2025.

602 CortexLM. MidJourney-V6 dataset. <https://huggingface.co/datasets/CortexLM/midjourney-v6>, 2025. Accessed: 2025-08-05.

604

605 Chaorui Deng, Deyao Zhu, Kunchang Li, Chenhui Gou, Feng Li, Zeyu Wang, Shu Zhong, Weihao
 606 Yu, Xiaonan Nie, Ziang Song, et al. Emerging properties in unified multimodal pretraining. *arXiv
 607 preprint arXiv:2505.14683*, 2025.

608 Patrick Esser, Sumith Kulal, Andreas Blattmann, Rahim Entezari, Jonas Müller, Harry Saini, Yam
 609 Levi, Dominik Lorenz, Axel Sauer, Frederic Boesel, et al. Scaling rectified flow transformers
 610 for high-resolution image synthesis. In *Forty-first international conference on machine learning*,
 611 2024.

612 Zhengcong Fei, Mingyuan Fan, Changqian Yu, Debang Li, Youqiang Zhang, and Junshi Huang.
 613 Dimba: Transformer-mamba diffusion models. *arXiv preprint arXiv:2406.01159*, 2024.

614

615 Chaoyou Fu, Peixian Chen, Yunhang Shen, Yulei Qin, Mengdan Zhang, Xu Lin, Jinrui Yang, Xiawu
 616 Zheng, Ke Li, Xing Sun, et al. Mme: A comprehensive evaluation benchmark for multimodal
 617 large language models. In *The Thirty-ninth Annual Conference on Neural Information Processing
 618 Systems Datasets and Benchmarks Track*, 2025.

619 Yuying Ge, Sijie Zhao, Chen Li, Yixiao Ge, and Ying Shan. Seed-data-edit technical report: A
 620 hybrid dataset for instructional image editing. *arXiv preprint arXiv:2405.04007*, 2024.

621

622 Dhruba Ghosh, Hannaneh Hajishirzi, and Ludwig Schmidt. Geneval: An object-focused framework
 623 for evaluating text-to-image alignment. *Advances in Neural Information Processing Systems*, 36:
 624 52132–52152, 2023.

625 Lixue Gong, Xiaoxia Hou, Fanshi Li, Liang Li, Xiaochen Lian, Fei Liu, Liyang Liu, Wei Liu,
 626 Wei Lu, Yichun Shi, et al. Seedream 2.0: A native chinese-english bilingual image generation
 627 foundation model. *arXiv preprint arXiv:2503.07703*, 2025.

628

629 Yash Goyal, Tejas Khot, Douglas Summers-Stay, Dhruv Batra, and Devi Parikh. Making the v in vqa
 630 matter: Elevating the role of image understanding in visual question answering. In *Proceedings
 631 of the IEEE conference on computer vision and pattern recognition*, pp. 6904–6913, 2017.

632 Dan Hendrycks, Collin Burns, Steven Basart, Andy Zou, Mantas Mazeika, Dawn Song, and
 633 Jacob Steinhardt. Measuring massive multitask language understanding. *arXiv preprint
 634 arXiv:2009.03300*, 2020.

635

636 Amir Hertz, Ron Mokady, Jay Tenenbaum, Kfir Aberman, Yael Pritch, and Daniel Cohen-Or.
 637 Prompt-to-prompt image editing with cross attention control. *arXiv preprint arXiv:2208.01626*,
 638 2022.

639 Wenyi Hong, Wenmeng Yu, Xiaotao Gu, Guo Wang, Guobing Gan, Haomiao Tang, Jiale Cheng,
 640 Ji Qi, Junhui Ji, Lihang Pan, et al. Glm-4.1 v-thinking: Towards versatile multimodal reasoning
 641 with scalable reinforcement learning. *arXiv e-prints*, pp. arXiv–2507, 2025.

642 Mude Hui, Siwei Yang, Bingchen Zhao, Yichun Shi, Heng Wang, Peng Wang, Yuyin Zhou, and
 643 Cihang Xie. Hq-edit: A high-quality dataset for instruction-based image editing. *arXiv preprint
 644 arXiv:2404.09990*, 2024.

645

646 Aaron Hurst, Adam Lerer, Adam P Goucher, Adam Perelman, Aditya Ramesh, Aidan Clark, AJ Os-
 647 trow, Akila Welihinda, Alan Hayes, Alec Radford, et al. Gpt-4o system card. *arXiv preprint
 648 arXiv:2410.21276*, 2024.

648 Aniruddha Kembhavi, Mike Salvato, Eric Kolve, Minjoon Seo, Hannaneh Hajishirzi, and Ali
 649 Farhadi. A diagram is worth a dozen images. In *European conference on computer vision*, pp.
 650 235–251. Springer, 2016.

651

652 Black Forest Labs. Flux. <https://github.com/black-forest-labs/flux>, 2024a.

653

654 Black Forest Labs. Flux. <https://github.com/black-forest-labs/flux>, 2024b.

655

656 Bo Li, Yuanhan Zhang, Dong Guo, Renrui Zhang, Feng Li, Hao Zhang, Kaichen Zhang, Peiyuan
 657 Zhang, Yanwei Li, Ziwei Liu, et al. Llava-onevision: Easy visual task transfer. *arXiv preprint*
 658 *arXiv:2408.03326*, 2024a.

659

660 Daiqing Li, Aleks Kamko, Ehsan Akhgari, Ali Sabet, Linmiao Xu, and Suhail Doshi. Playground
 661 v2. 5: Three insights towards enhancing aesthetic quality in text-to-image generation. *arXiv*
 662 *preprint arXiv:2402.17245*, 2024b.

663

664 Bin Lin, Zongjian Li, Xinhua Cheng, Yuwei Niu, Yang Ye, Xianyi He, Shenghai Yuan, Wangbo Yu,
 665 Shaodong Wang, Yunyang Ge, et al. Uniworld: High-resolution semantic encoders for unified
 666 visual understanding and generation. *arXiv preprint arXiv:2506.03147*, 2025.

667

668 Tsung-Yi Lin, Michael Maire, Serge Belongie, James Hays, Pietro Perona, Deva Ramanan, Piotr
 669 Dollár, and C Lawrence Zitnick. Microsoft coco: Common objects in context. In *European*
 670 *conference on computer vision*, pp. 740–755. Springer, 2014.

671

672 Haotian Liu, Chunyuan Li, Qingyang Wu, and Yong Jae Lee. Visual instruction tuning. *Advances*
 673 *in neural information processing systems*, 36:34892–34916, 2023a.

674

675 Shiyu Liu, Yucheng Han, Peng Xing, Fukun Yin, Rui Wang, Wei Cheng, Jiaqi Liao, Yingming
 676 Wang, Honghao Fu, Chunrui Han, et al. Step1x-edit: A practical framework for general image
 677 editing. *arXiv preprint arXiv:2504.17761*, 2025.

678

679 Yuliang Liu, Zhang Li, Hongliang Li, Wenwen Yu, Mingxin Huang, Dezhi Peng, Mingyu Liu,
 680 Mingrui Chen, Chunyuan Li, Lianwen Jin, et al. On the hidden mystery of ocr in large multimodal
 681 models. *arXiv preprint arXiv:2305.07895*, 2(5):6, 2023b.

682

683 Pan Lu, Hritik Bansal, Tony Xia, Jiacheng Liu, Chunyuan Li, Hannaneh Hajishirzi, Hao Cheng, Kai-
 684 Wei Chang, Michel Galley, and Jianfeng Gao. Mathvista: Evaluating mathematical reasoning of
 685 foundation models in visual contexts. *arXiv preprint arXiv:2310.02255*, 2023.

686

687 Yujie Lu, Dongfu Jiang, Wenhui Chen, William Yang Wang, Yejin Choi, and Bill Yuchen Lin. Wild-
 688 vision: Evaluating vision-language models in the wild with human preferences. *Advances in*
 689 *Neural Information Processing Systems*, 37:48224–48255, 2024.

690

691 Chaojie Mao, Jingfeng Zhang, Yulin Pan, Zeyinzi Jiang, Zhen Han, Yu Liu, and Jingren Zhou.
 692 Ace++: Instruction-based image creation and editing via context-aware content filling. *arXiv*
 693 *preprint arXiv:2501.02487*, 2025.

694

695 Kenneth Marino, Mohammad Rastegari, Ali Farhadi, and Roozbeh Mottaghi. Ok-vqa: A visual
 696 question answering benchmark requiring external knowledge. In *Proceedings of the IEEE/cvf*
 697 *conference on computer vision and pattern recognition*, pp. 3195–3204, 2019.

698

699 Ahmed Masry, Xuan Long Do, Jia Qing Tan, Shafiq Joty, and Enamul Hoque. Chartqa: A bench-
 700 mark for question answering about charts with visual and logical reasoning. In *Findings of the*
 701 *association for computational linguistics: ACL 2022*, pp. 2263–2279, 2022.

702

703 Minesh Mathew, Dimosthenis Karatzas, and CV Jawahar. Docvqa: A dataset for vqa on document
 704 images. In *Proceedings of the IEEE/CVF winter conference on applications of computer vision*,
 705 pp. 2200–2209, 2021.

706

707 OpenAI. Introducing 4o image generation. <https://openai.com/index/introducing-4o-image-generation/>, March 25 2025. Accessed: YYYY-MM-
 708 DD.

702 Xichen Pan, Satya Narayan Shukla, Aashu Singh, Zhuokai Zhao, Shlok Kumar Mishra, Jialiang
 703 Wang, Zhiyang Xu, Juhai Chen, Kunpeng Li, Felix Juefei-Xu, et al. Transfer between modalities
 704 with metaqueries. *arXiv preprint arXiv:2504.06256*, 2025.

705 Sayak Paul. Flux.1-dev-edit-v0. <https://huggingface.co/sayakpaul/FLUX.1-dev-edit-v0>, 2025.

708 Dustin Podell, Zion English, Kyle Lacey, Andreas Blattmann, Tim Dockhorn, Jonas Müller, Joe
 709 Penna, and Robin Rombach. Sdxl: Improving latent diffusion models for high-resolution image
 710 synthesis. *arXiv preprint arXiv:2307.01952*, 2023.

711 Yusu Qian, Hanrong Ye, Jean-Philippe Fauconnier, Peter Grasch, Yinfei Yang, and Zhe Gan. Mia-
 712 bench: Towards better instruction following evaluation of multimodal llms. *arXiv preprint*
 713 *arXiv:2407.01509*, 2024.

714 David Rein, Betty Li Hou, Asa Cooper Stickland, Jackson Petty, Richard Yuanzhe Pang, Julien Di-
 715 rani, Julian Michael, and Samuel R Bowman. Gpqa: A graduate-level google-proof q&a bench-
 716 mark. In *First Conference on Language Modeling*, 2024.

718 Oleksii Sidorov, Ronghang Hu, Marcus Rohrbach, and Amanpreet Singh. Textcaps: a dataset for
 719 image captioning with reading comprehension. In *European conference on computer vision*, pp.
 720 742–758. Springer, 2020.

722 Amanpreet Singh, Vivek Natarajan, Meet Shah, Yu Jiang, Xinlei Chen, Dhruv Batra, Devi Parikh,
 723 and Marcus Rohrbach. Towards vqa models that can read. In *Proceedings of the IEEE/CVF*
 724 *conference on computer vision and pattern recognition*, pp. 8317–8326, 2019.

725 Keqiang Sun, Junting Pan, Yuying Ge, Hao Li, Haodong Duan, Xiaoshi Wu, Renrui Zhang, Aojuun
 726 Zhou, Zipeng Qin, Yi Wang, et al. Journeydb: A benchmark for generative image understanding.
 727 *Advances in neural information processing systems*, 36:49659–49678, 2023.

729 Jiangshan Wang, Junfu Pu, Zhongang Qi, Jiayi Guo, Yue Ma, Nisha Huang, Yuxin Chen, Xiu Li,
 730 and Ying Shan. Taming rectified flow for inversion and editing. *arXiv preprint arXiv:2411.04746*,
 731 2024a.

732 Weiyun Wang, Zhangwei Gao, Lixin Gu, Hengjun Pu, Long Cui, Xingguang Wei, Zhaoyang Liu,
 733 Linglin Jing, Shenglong Ye, Jie Shao, et al. Internvl3. 5: Advancing open-source multimodal
 734 models in versatility, reasoning, and efficiency. *arXiv preprint arXiv:2508.18265*, 2025.

735 Xinlong Wang, Xiaosong Zhang, Zhengxiong Luo, Quan Sun, Yufeng Cui, Jinsheng Wang, Fan
 736 Zhang, Yueze Wang, Zhen Li, Qiyi Yu, et al. Emu3: Next-token prediction is all you need.
 737 *arXiv preprint arXiv:2409.18869*, 2024b.

739 Chengyue Wu, Xiaokang Chen, Zhiyu Wu, Yiyang Ma, Xingchao Liu, Zizheng Pan, Wen Liu,
 740 Zhenda Xie, Xingkai Yu, Chong Ruan, et al. Janus: Decoupling visual encoding for unified
 741 multimodal understanding and generation. In *Proceedings of the Computer Vision and Pattern*
 742 *Recognition Conference*, pp. 12966–12977, 2025a.

743 Size Wu, Zhonghua Wu, Zerui Gong, Qingyi Tao, Sheng Jin, Qinyue Li, Wei Li, and Chen Change
 744 Loy. Openuni: A simple baseline for unified multimodal understanding and generation. *arXiv*
 745 *preprint arXiv:2505.23661*, 2025b.

746 xAI. Realworldqa, 2024. URL <https://x.ai/blog/grok-1.5-vision-preview>.

748 Shitao Xiao, Yueze Wang, Junjie Zhou, Huaying Yuan, Xingrun Xing, Ruiran Yan, Chaofan Li,
 749 Shuting Wang, Tiejun Huang, and Zheng Liu. Omnigen: Unified image generation. In *Proceed-
 750 ings of the Computer Vision and Pattern Recognition Conference*, pp. 13294–13304, 2025.

751 LLM-Core-Team Xiaomi. Mimo-vl technical report, 2025. URL <https://arxiv.org/abs/2506.03569>.

754 Enze Xie, Junsong Chen, Yuyang Zhao, Jincheng Yu, Ligeng Zhu, Chengyue Wu, Yujun Lin, Zhekai
 755 Zhang, Muyang Li, Junyu Chen, et al. Sana 1.5: Efficient scaling of training-time and inference-
 time compute in linear diffusion transformer. *arXiv preprint arXiv:2501.18427*, 2025a.

756 Jinheng Xie, Weijia Mao, Zechen Bai, David Junhao Zhang, Weihao Wang, Kevin Qinghong Lin,
 757 Yuchao Gu, Zhijie Chen, Zhenheng Yang, and Mike Zheng Shou. Show-o: One single transformer
 758 to unify multimodal understanding and generation. *arXiv preprint arXiv:2408.12528*, 2024.
 759

760 Jinheng Xie, Zhenheng Yang, and Mike Zheng Shou. Show-o2: Improved native unified multimodal
 761 models. *arXiv preprint arXiv:2506.15564*, 2025b.
 762

763 Kaining Ying, Fanqing Meng, Jin Wang, Zhiqian Li, Han Lin, Yue Yang, Hao Zhang, Wenbo Zhang,
 764 Yuqi Lin, Shuo Liu, et al. Mmt-bench: A comprehensive multimodal benchmark for evaluating
 765 large vision-language models towards multitask agi. *arXiv preprint arXiv:2404.16006*, 2024.
 766

767 Qifan Yu, Wei Chow, Zhongqi Yue, Kaihang Pan, Yang Wu, Xiaoyang Wan, Juncheng Li, Siliang
 768 Tang, Hanwang Zhang, and Yueting Zhuang. Anyedit: Mastering unified high-quality image
 769 editing for any idea. In *Proceedings of the Computer Vision and Pattern Recognition Conference*,
 pp. 26125–26135, 2025.
 770

771 Weihao Yu, Zhengyuan Yang, Linjie Li, Jianfeng Wang, Kevin Lin, Zicheng Liu, Xinchao Wang,
 772 and Lijuan Wang. Mm-vet: Evaluating large multimodal models for integrated capabilities. *arXiv
 preprint arXiv:2308.02490*, 2023.
 773

774 Weihao Yu, Zhengyuan Yang, Lingfeng Ren, Linjie Li, Jianfeng Wang, Kevin Lin, Chung-Ching
 775 Lin, Zicheng Liu, Lijuan Wang, and Xinchao Wang. Mm-vet v2: A challenging benchmark to
 776 evaluate large multimodal models for integrated capabilities. *arXiv preprint arXiv:2408.00765*,
 777 2024.
 778

779 Xiang Yue, Yuansheng Ni, Kai Zhang, Tianyu Zheng, Ruoqi Liu, Ge Zhang, Samuel Stevens,
 780 Dongfu Jiang, Weiming Ren, Yuxuan Sun, et al. Mmmu: A massive multi-discipline multi-
 781 modal understanding and reasoning benchmark for expert agi. In *Proceedings of the IEEE/CVF
 Conference on Computer Vision and Pattern Recognition*, pp. 9556–9567, 2024.
 782

783 Xiang Yue, Tianyu Zheng, Yuansheng Ni, Yubo Wang, Kai Zhang, Shengbang Tong, Yuxuan Sun,
 784 Botao Yu, Ge Zhang, Huan Sun, et al. Mmmu-pro: A more robust multi-discipline multimodal
 785 understanding benchmark. In *Proceedings of the 63rd Annual Meeting of the Association for
 Computational Linguistics (Volume 1: Long Papers)*, pp. 15134–15186, 2025.
 786

787 Kai Zhang, Lingbo Mo, Wenhui Chen, Huan Sun, and Yu Su. Magicbrush: A manually annotated
 788 dataset for instruction-guided image editing. *Advances in Neural Information Processing Systems*,
 36:31428–31449, 2023.
 789

790 Zechuan Zhang, Ji Xie, Yu Lu, Zongxin Yang, and Yi Yang. Enabling instructional image edit-
 791 ing with in-context generation in large scale diffusion transformer. In *The Thirty-ninth Annual
 792 Conference on Neural Information Processing Systems*, 2025.
 793

794 Haozhe Zhao, Xiaojian Shawn Ma, Liang Chen, Shuzheng Si, Rujie Wu, Kaikai An, Peiyu Yu,
 795 Minjia Zhang, Qing Li, and Baobao Chang. Ultraedit: Instruction-based fine-grained image
 796 editing at scale. *Advances in Neural Information Processing Systems*, 37:3058–3093, 2024.
 797

798 Jeffrey Zhou, Tianjian Lu, Swaroop Mishra, Siddhartha Brahma, Sujoy Basu, Yi Luan, Denny
 Zhou, and Le Hou. Instruction-following evaluation for large language models. *arXiv preprint
 arXiv:2311.07911*, 2023.
 800
 801
 802
 803
 804
 805
 806
 807
 808
 809

810 A ADDITIONAL EXPERIMENTS
811
812813 Table 11: The overall image editing performance on **GEdit-Bench-EN**. We use GPT-4.1 for eval-
814 uation to ensure consistency with the existing results reported in Step1X-Edit. * indicates results
815 evaluated by us. SC and PQ denote Semantic Consistency and Perceptual Quality, respectively.
816

817 Model	Intersection subset			Full set		
	818 SC	PQ	Overall	819 SC	PQ	Overall
<i>Proprietary Models</i>						
Gemini (Comanici et al., 2025)	6.82	7.41	6.48	6.87	7.44	6.51
GPT-4o (OpenAI, 2025)	7.40	7.90	7.14	7.22	7.89	6.98
Doubao (Gong et al., 2025)	7.87	8.10	7.59	7.74	8.13	7.49
<i>Open-Source Models</i>						
Instruct-P2P (Brooks et al., 2023)	3.34	6.21	3.23	3.30	6.19	3.22
MagicBrush (Zhang et al., 2023)	4.56	6.34	4.24	4.52	6.37	4.19
AnyEdit (Yu et al., 2025)	3.12	5.87	2.92	3.05	5.88	2.85
OmniGen (Xiao et al., 2025)	6.04	5.86	5.15	5.88	5.87	5.01
UniWorld-V1 (Lin et al., 2025)	-	-	-	4.93	7.43	4.85
Janus-4o* (Chen et al., 2025b)	4.69	4.68	3.91	4.64	4.57	3.83
Step1X-Edit (Liu et al., 2025)	7.29	6.96	6.62	7.13	7.00	6.44
DIM-4.6B-Edit	6.91	6.90	6.46	6.65	6.71	6.18

830
831
832 Table 12: The detailed task-wise performance on **GEdit-Bench-EN** Full set. * indicates results eval-
833 uated by us. Task abbreviations: Background Change (BC), Color Alter (CA), Material Alter (MA),
834 Motion Change (MC), PS Human (PH), Style Change (SC), Subject-Add (SA), Subject-Remove
835 (SRM), Subject-Replace (SRP), Text Change (TC), Tone Transfer (TT), and Average (AVG).
836

837 Model	BC	CA	MA	MC	PH	SC	SA	SRM	SRP	TC	TT	AVG	AVG w/o TC
<i>Semantic Consistency</i>													
UniWorld-V1	5.17	7.21	4.71	1.14	3.49	5.98	7.42	6.50	6.04	1.07	5.52	4.93	5.32
Janus-4o*	5.48	6.68	6.00	2.75	4.04	8.03	5.10	1.74	4.27	2.11	4.88	4.64	4.90
Step1X-Edit	8.40	7.68	7.95	3.40	5.06	8.13	7.92	6.88	8.27	7.72	7.05	7.13	7.07
DIM-4.6B-Edit	7.68	7.65	7.48	4.78	5.64	8.22	8.10	7.05	7.45	2.34	6.73	6.65	7.08
<i>Perceptual Quality</i>													
UniWorld-V1	7.59	6.82	6.86	8.68	8.61	6.58	7.61	7.28	6.78	7.44	7.48	7.43	7.43
Janus-4o*	4.00	4.20	4.08	5.73	6.07	4.40	4.77	4.07	4.72	4.44	3.78	4.57	4.58
Step1X-Edit	6.40	6.10	5.60	7.63	8.31	6.75	7.27	7.49	6.85	7.86	6.73	7.00	6.91
DIM-4.6B-Edit	6.73	6.55	5.13	7.15	7.43	6.53	7.28	6.83	6.65	6.61	6.88	6.71	6.71
<i>Overall</i>													
UniWorld-V1	4.92	6.37	4.79	1.85	4.03	5.64	7.23	6.17	5.70	1.15	5.54	4.85	5.22
Janus-4o*	4.31	5.02	4.41	2.71	4.09	5.80	4.07	1.69	3.69	2.35	3.96	3.83	3.97
Step1X-Edit	7.03	6.26	6.46	3.66	5.23	7.24	7.17	6.42	7.39	7.40	6.62	6.44	6.35
DIM-4.6B-Edit	7.02	6.81	6.00	4.67	5.88	7.16	7.48	6.67	6.76	2.99	6.55	6.18	6.50

847
848
849
850
851
852
853
854 Table 13: The generation configuration and inference speed of Step1X-Edit and DIM-4.6B-Edit.
855

856 Model	Gen. Resolution	Gen. Steps	Und. Params	Gen. Params	VAE Rate	Prompt	Speed
Step1X-Edit	1024×1024	30	7B	12.5B	8×	Raw	28.19s
DIM-4.6B-Edit			3B	1.6B	32×	CoT	6.23s

859
860 **Detailed Performance on GEdit-Bench-EN.** Table 11 and 12 summarize overall and detailed task-
861 wise performance of different models on GEdit-Bench-EN, respectively. Our DIM-4.6B-Edit ranks
862 just behind the in-domain tester, *i.e.*, Step1X-Edit, while surpassing all other out-of-domain com-
863 petitors. Moreover, among out-of-domain testers, DIM-4.6B-Edit is the only model that consistently
preserves both semantic consistency and perceptual quality. This demonstrates the effectiveness of

864
865 Table 14: **The ImgEdit performance of different models with/without using DIM CoT as instruction.**
866

Model	Params	CoT	Add	Adjust	Extract	Replace	Remove	Background	Style	Hybrid	Action	Overall
DIM-4.6B-Edit	Und  Gen 		3.53	3.23	2.01	3.49	1.47	3.42	4.79	2.35	3.64	3.10
			4.09	3.47	2.30	4.00	3.43	3.87	4.92	2.85	4.08	3.67
Janus-4o	Und  Gen 		3.35	3.35	2.25	3.01	2.18	3.32	4.71	2.49	4.04	3.19
			3.95	2.74	2.49	3.59	2.28	3.31	4.72	2.62	4.02	3.30
Step1X-Edit	Und  Gen 		3.88	3.14	1.76	3.40	2.41	3.16	4.63	2.64	2.52	3.06
			3.56	2.47	1.81	3.13	2.02	2.84	4.18	1.80	2.46	2.70

872
873 Table 15: **The performance of DIM-4.6B-T2I/Edit on understanding benchmarks.**
874

Model	Params	MME-P	MMB	SEED	MMMU	MM-Vet
Janus (Wu et al., 2025a)	1.3B 	1338.0	69.4	63.7	30.5	34.3
Emu3-Gen (Wang et al., 2024b)	8.0B 	-	58.5	68.2	31.6	37.2
Show-o (Xie et al., 2024)	1.3B 	1097.2	-	-	26.7	-
Show-o2-7B (Xie et al., 2025b)	7.0B 	1620.5	79.3	69.8	48.9	-
Janus-Pro-7B (Chen et al., 2025c)	7.0B 	1567.1	79.2	72.1	41.0	50.0
BAGEL (Deng et al., 2025)	14.0B 	1687.0	85.0	-	55.3	67.2
MetaQuery-L (Pan et al., 2025)	3.0B  3.2B 	1574.3	78.6	73.8	53.1	63.2
DIM-4.6B-T2I/Edit	3.0B  1.6B 	1574.3	78.6	73.8	53.1	63.2

884
885 DIM-Edit, where edits with high perceptual fidelity are precisely aligned with CoT-style imagination,
886 thereby ensuring semantic correctness.
887888 **Inference Efficiency.** Beyond precise image editing, our DIM-4.6B-Edit also maintains highly
889 efficient inference inherited from the SANA architecture. To verify this, we compare the average
890 editing time over 100 samples between Step1X-Edit and DIM-4.6B-Edit, as reported in Table 13.
891 Specifically, Step1X-Edit is provided with short raw prompts, while DIM-4.6B-Edit is evaluated
892 with longer CoT prompts. Even under this more demanding setting, our model achieves a $4.5 \times$
893 speedup while preserving high editing quality, highlighting the effectiveness of the proposed DIM
894 dataset and the Draw-In-Mind paradigm.
895896 **Impact of DIM CoT for Different Models.** To investigate the impact of DIM-style CoT on different
897 models, we evaluated the performance of Janus-4o and Step1X-Edit when directly provided with the
898 same CoT blueprints as input instructions on ImgEdit. The results are presented in Table 14. Based
899 on these results, we have the following observations and analysis:
900

- DIM-4.6B-Edit is explicitly trained on complex CoT-style blueprints from the DIM-Edit dataset, it achieves superior CoT comprehension. Consequently, it demonstrates substantial performance gains when DIM-style CoTs are applied during inference.
- Janus-4o employs an end-to-end fine-tuning approach, which minimizes the gap between instruction understanding and generation. This makes it more robust to input distribution shifts. While it possesses mild CoT comprehension capabilities and benefits slightly from DIM-style CoTs, the performance gain is less pronounced compared to DIM-4.6B-Edit.
- Step1X-Edit adopts a training recipe similar to ours (using a frozen understanding core), this design makes it susceptible to input distribution shifts when facing unseen instruction formats. It struggles to process CoT inputs effectively, leading to performance degradation when DIM-style CoTs are applied.

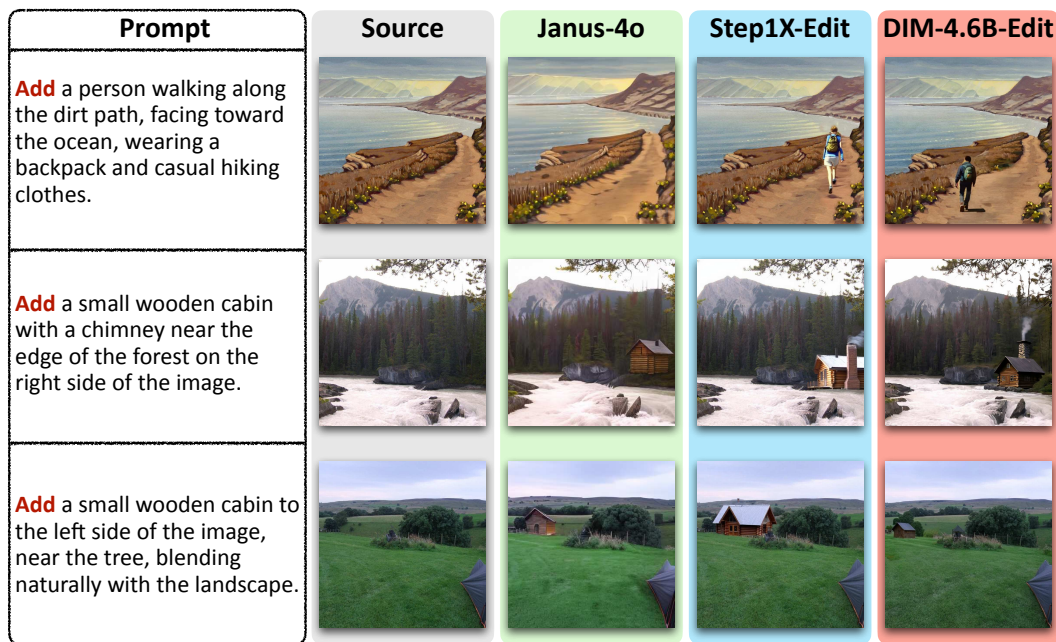
910 Based on these findings, we conclude that *superior CoT comprehension is pivotal for enhancing*
911 *editing performance.* This finding validates our strategy of fostering CoT comprehension by
912 constructing DIM-T2I and utilizing DIM-4.6B-T2I as the initialization for the editing task.
913914 **Understanding Performance.** Since the MLLM component is frozen during DIM training, its under-
915 standing performance remains unaffected and is identical to the results reported in the original
916 paper. To ensure clarity regarding the model’s capabilities, we report the corresponding understand-
917 ing performance in Table 15. Our experiments demonstrate that DIM-4.6B-Edit achieves superior
918 editing performance even when utilizing a relatively small MLLM under a frozen setting. *This find-*

918
 919 *ing highlights the flexibility of our approach: users can seamlessly upgrade to advanced MLLMs to*
 920 *unlock even greater understanding and editing performance. Such integration is straightforward, as*
 921 *our streamlined architecture and training recipe avoid the need for intricate parameter tuning.*

922 B ADDITIONAL VISUALIZATIONS

923 B.1 VISUALIZATION OF DIFFERENT EDITING OPERATIONS.

926 Beyond Figure 3 in the manuscript, we further visualize the edits of Janus-4o, Step1X-Edit, and
 927 our DIM-4.6B-Edit under the operations of *add*, *change*, *remove*, *replace*, and *style transfer* in
 928 Figure 4, 5, 6, 7, and 8, respectively. As shown, DIM-4.6B-Edit consistently preserves the overall
 929 layout while performing natural edits. For instance, in Figure 4, Janus-4o fails to generate details
 930 of the wooden cabin, while Step1X-Edit places the chimney on the river, which is counterfactual.
 931 In contrast, our DIM-4.6B-Edit carefully adds the wooden cabin while ensuring naturalness. In
 932 Figure 5, Janus-4o fails to follow the color change instruction. Step1X-Edit changes the singer’s
 933 shirt to blue but also alters fine details such as the collar shape. By comparison, our DIM-4.6B-
 934 Edit changes the shirt to red while preserving all details, including the shadow cast by the hand. In
 935 Figure 6, both DIM-4.6B-Edit and Step1X-Edit perform successful removals, whereas Janus-4o fails
 936 to remove the seaplane. In Figure 7, only DIM-4.6B-Edit captures the semantics of “majestically”
 937 and generates a roaring lion. Finally, in Figure 8, although all three models succeed in style transfer,
 938 only DIM-4.6B-Edit captures subtle visual cues, such as the green grass in the last row, and repaints
 939 them faithfully in the edits.



961 Figure 4: The edits of **Janus-4o**, **Step1X-Edit**, and **DIM-4.6B-Edit** for the *add* operation.
 962

972
973
974
975
976
977
978
979
980
981
982
983
984
985
986
987
988
989
990
991
992
993
994

Prompt	Source	Janus-4o	Step1X-Edit	DIM-4.6B-Edit
Change the person's shirt color to blue.				
Change the animal's fur color to a solid shade of brown.				
Change the background from the snow to a beach setting.				

Figure 5: The edits of **Janus-4o**, **Step1X-Edit**, and **DIM-4.6B-Edit** for the *change* operation.

1000
1001
1002
1003
1004
1005
1006
1007
1008
1009
1010
1011
1012
1013
1014
1015
1016
1017
1018
1019
1020
1021
1022

Prompt	Source	Janus-4o	Step1X-Edit	DIM-4.6B-Edit
Remove the child standing near the edge of the water.				
Remove the sheep in the foreground.				
Remove the seaplane on the shoreline.				

Figure 6: The edits of **Janus-4o**, **Step1X-Edit**, and **DIM-4.6B-Edit** for the *remove* operation.

1023
1024
1025

1026

1027

1028

1029

1030 **Replace** the deer in the
 1031 image with a lion standing
 1032 majestically in the same
 1033 forest setting, under the
 1034 glowing golden light and light
 1035 snowflakes.

1036

1037

1038

1039 **Replace** the mountain goat in
 1040 the image with a rabbit.

1041

1042

1043

1044 **Replace** the horse in the
 1045 image with a cat.

1046

1047

1048

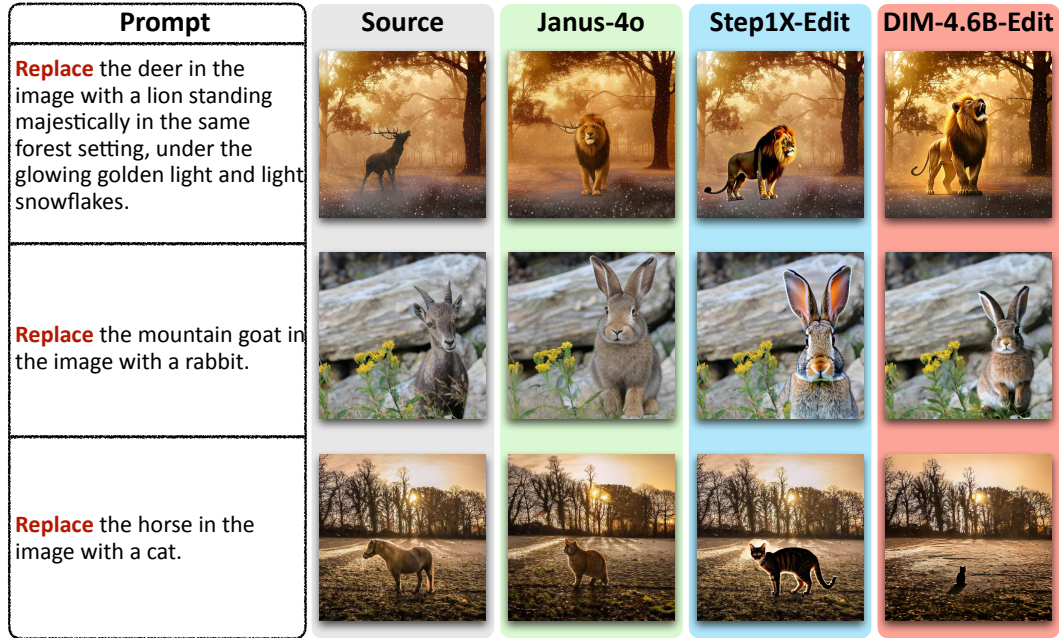


Figure 7: The edits of **Janus-4o**, **Step1X-Edit**, and **DIM-4.6B-Edit** for the *replace* operation.

1049

1050

1051

1052

1053

1054

1055

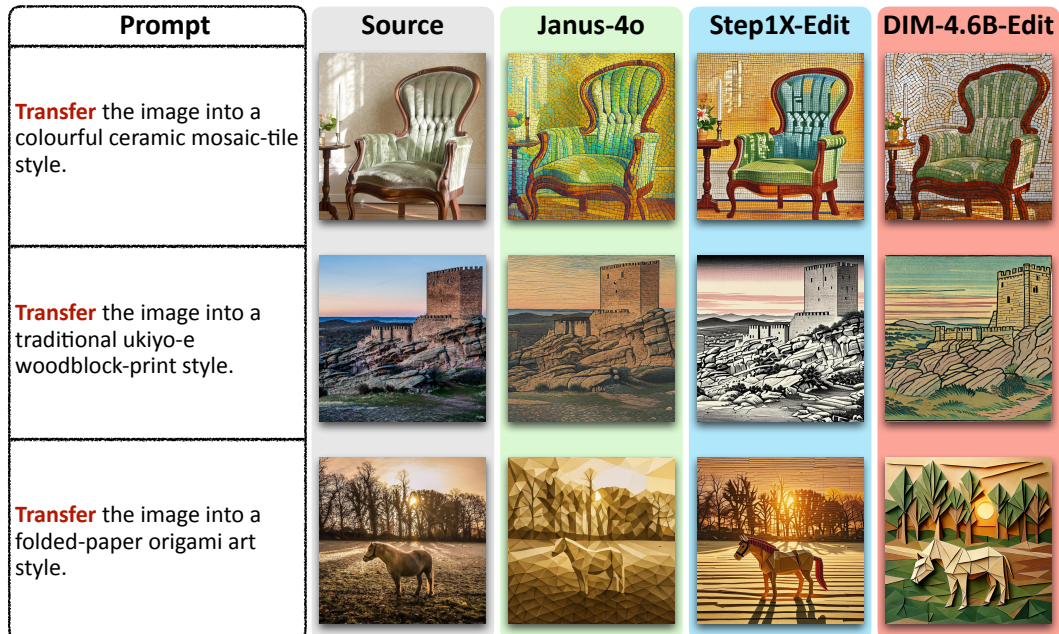


Figure 8: The edits of **Janus-4o**, **Step1X-Edit**, and **DIM-4.6B-Edit** for *style transfer*.

1077

1078

1079

1080

1081

1082

B.2 VISUALIZATION OF THE DRAW-IN-MIND WORKFLOW’S IMPACT ON IMAGE EDITING.

1083

1084

1085

1086

1087

1088

Relying solely on numerical metrics may not intuitively convey the practical impact of the Draw-In-Mind workflow on image generation. To address this, we present Figure 9, 10, 11, 12, and 13 to showcase several advanced usage scenarios. These examples demonstrate complex cases that are successfully handled by DIM-Edit-4.6B, highlighting capabilities that remain beyond the reach of current baseline methods.

1089

1090

1091

1092

1093

1094

1095

1096

1097

Instruction Disambiguation. In Figure 9, the user instruction presents an inherent ambiguity due to the presence of three lemons on the table. This task necessitates precise multi-object localization and removal, which is a challenge that proves difficult without the Draw-In-Mind paradigm, as standard models often struggle with the required multi-object reasoning. Consequently, both the 7B Janus-4o and 12B Step1X-Edit fail to execute the edit correctly. Similarly, when CoT is disabled, our DIM-4.6B-Edit also fails to remove all targets. However, with DIM CoT enabled, the generated design blueprints effectively disambiguate the instruction. They accurately localize the three lemons to the right of the vase and ensure their complete removal, while perfectly preserving the integrity of the unedited regions.

1098

1099

1100

1101

1102

1103

1104

1105

1106

Edit Navigation and Structural Planning. In Figure 10, the user instruction presents two distinct challenges: **(i)** determining the optimal placement for a wooden cabin, and **(ii)** identifying the appropriate structural integration for a chimney. These dual requirements impose a significant burden on the generation model. Consequently, in Janus-4o’s output, the chimney is nearly invisible, while Step1X-Edit places the cabin counterintuitively close to the river. Similarly, DIM without CoT fails to simultaneously resolve the cabin placement and chimney addition. In contrast, DIM powered by CoT effectively navigates these challenges. It observes that “the trees thin out on the right side” (GLP) and selects this area as the optimal location (EAL). It then explicitly envisions the cabin’s appearance, including a chimney emitting smoke (EII), ultimately yielding the most plausible and high-quality edit among all competitors.

1107

1108

1109

1110

1111

1112

1113

Commonsense-guarded Editing. In Figure 11, the editing task presents a subtle complexity: it requires commonsense reasoning regarding scale. From the same viewpoint, a cat should appear significantly smaller than a horse. All baseline models, including our own DIM w/o CoT, overlook this physical constraint, simply replacing the horse with a cat of identical dimensions. In contrast, DIM with CoT successfully leverages commonsense reasoning. It recognizes the size discrepancy and executes a “commonsense-guarded” edit, placing a naturally scaled cat at the target location, thereby preserving scene realism.

1114

1115

1116

1117

1118

Advanced Causal Editing. In Figure 12, we present an advanced causal editing scenario where the instruction implies the target quantity (referencing “the second prime number”) rather than stating it explicitly. Unsurprisingly, all baseline models fail to resolve this implicit requirement. In contrast, DIM with CoT swiftly infers the correct number of cherries and executes a successful edit, demonstrating its ability to handle knowledge-intensive instructions.

1119

1120

1121

1122

1123

Advanced Temporal Editing. Figure 13 illustrates the most complex temporal editing scenario, which necessitates a deep understanding of chemical reaction dynamics. Similar to the previous example, none of the baseline models succeed in this task. In contrast, DIM with CoT accurately characterizes the reaction process and executes physically plausible edits, demonstrating its capability to handle sophisticated temporal reasoning.

1124

1125

1126

1127

1128

1129

1130

1131

1132

1133

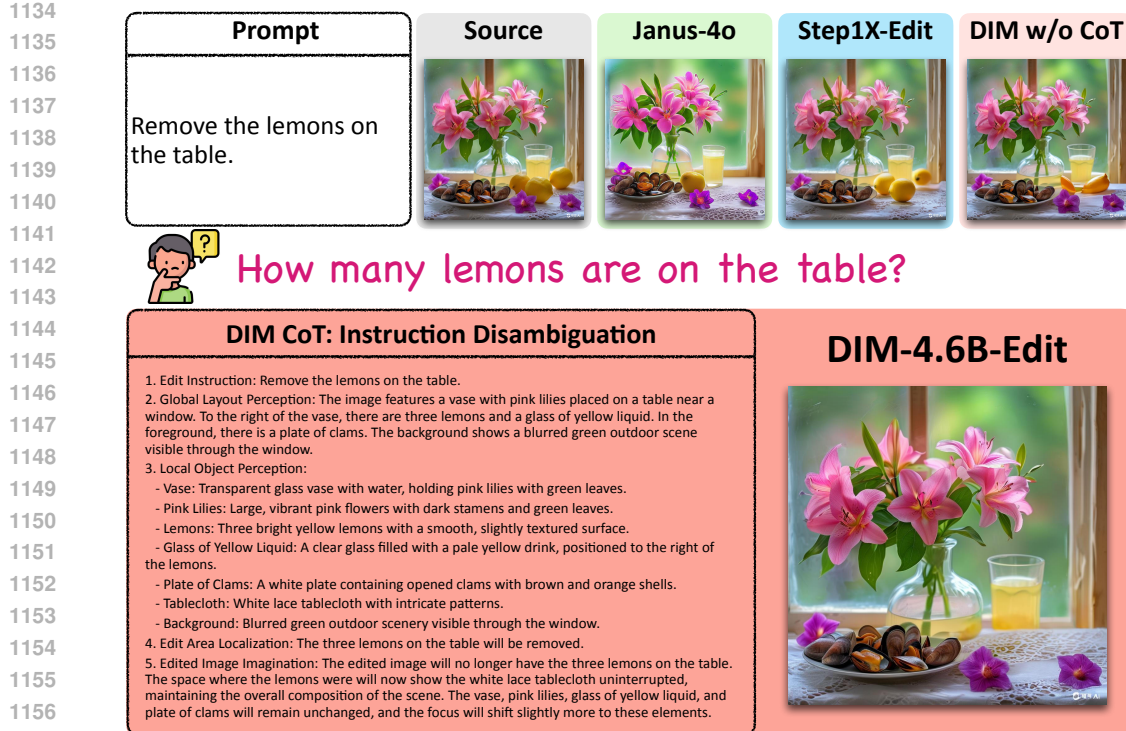


Figure 9: The edits of **Janus-4o**, **Step1X-Edit**, **DIM w/o CoT**, and **DIM-4.6B-Edit** when the user instruction is ambiguous. DIM CoT is capable of *instruction disambiguation* under this case.

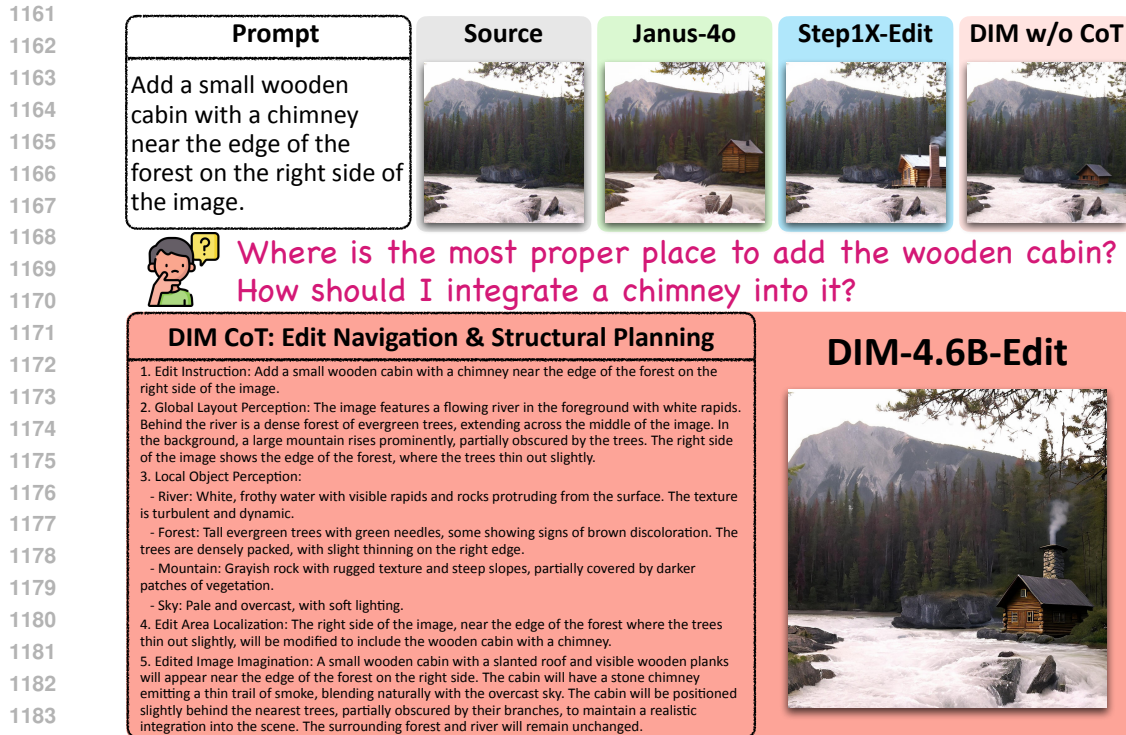


Figure 10: The edits of **Janus-4o**, **Step1X-Edit**, **DIM w/o CoT**, and **DIM-4.6B-Edit** when the user instruction requires localization and involves fine-grained structure modification. DIM CoT is capable of *edit navigation and structural planning* under this case.

1188
1189
1190
1191
1192
1193
1194
1195
1196
1197



From the same viewpoint, the cat should be much smaller than the horse...

1198
1199
1200
1201
1202
1203
1204
1205
1206
1207
1208
1209
1210
1211

DIM CoT: Commonsense-guarded Editing

1. Edit Instruction: Replace the horse in the image with a cat.
 2. Global Layout Perception: The image features a horse standing in a grassy field. The field is covered with frost and scattered leaves. In the background, there is a line of tall, leafless trees, and the sun is shining through the trees, creating long shadows across the ground.
 3. Local Object Perception:
 - Horse: Positioned slightly left of center, the horse is light beige in color with a smooth texture and a visible harness. It is standing still, facing slightly to the left.
 - Field: The ground is covered with frosty grass and scattered brown leaves, giving it a textured appearance.
 - Trees: Tall, leafless trees with intricate branches form the background. They are dark brown and silhouetted against the bright sunlight.
 - Sunlight: The sun is low in the sky, casting warm golden light and long shadows across the field.
 4. Edit Area Localization: The horse will be replaced with a cat. The area of change is the space occupied by the horse, including its immediate surroundings to ensure the cat is seamlessly integrated into the scene.
 5. Edited Image Imagination: The horse is replaced by a cat, which is smaller in size and positioned in the same area slightly left of center. The cat is sitting or standing, with fur that could be a similar beige color to match the lighting and overall tone of the image. The frosty field, trees, and sunlight remain unchanged, with the cat casting a smaller shadow on the ground due to its size. The scene retains its tranquil and warm atmosphere.

DIM-4.6B-Edit



1212
1213
1214
1215

Figure 11: The edits of **Janus-4o**, **Step1X-Edit**, **DIM w/o CoT**, and **DIM-4.6B-Edit** when the user instruction involves implicit commonsense constraint. DIM CoT is capable of *commonsense-guarded editing* under this case.

1216
1217
1218
1219
1220
1221
1222
1223
1224



Which number is the second prime number?

1225
1226
1227
1228
1229
1230
1231
1232
1233
1234
1235
1236
1237
1238
1239

DIM CoT: Advanced Causal Editing

1. Edit Instruction: Generate this still-life scene with cherries visible totaling the second prime number.
 2. Global Layout Perception: The image depicts a still-life arrangement. Key objects include:
 - A glass goblet with a spiral lemon peel draped over it, located in the upper left quadrant.
 - A cluster of white grapes, positioned centrally and spilling slightly to the left.
 - Two lemons, one whole and one partially sliced, located in the lower left quadrant.
 - A large yellow fruit (possibly a grapefruit or melon) in the upper center-right.
 - A cluster of cherries, located in the lower right quadrant.
 - A green fabric draped over the table, forming the base of the composition.
 - A wooden table surface visible in the lower right corner.
 - Grape leaves and vines extending from the fruit, adding a naturalistic touch.
 3. Local Object Perception:
 - **Glass goblet**: Transparent, reflective, and elevated, with a spiral lemon peel (yellow, textured) hanging from it.
 - **White grapes**: Round, translucent, and glossy, with a pale greenish-white hue.
 - **Lemons**: Bright yellow with a textured rind; one is whole, and the other is sliced to reveal its juicy interior.
 - **Large yellow fruit**: Smooth, round, and slightly textured, with a vibrant yellow color.
 - **Cherries**: Small, round, and glossy, with a deep red hue and attached stems.
 - **Green fabric**: Rich green, with folds and a soft texture, reflecting light.
 - **Wooden table**: Brown, with a smooth surface and visible grain.
 - **Grape leaves and vines**: Green and brown, with a natural, organic shape and texture.
 4. Edit Area Localization: The cluster of cherries in the lower right quadrant will be modified. The number of cherries will be adjusted to total the second prime number, which is 3.
 5. Edited Image Imagination: The edited image will feature the same still-life arrangement, but the cluster of cherries in the lower right quadrant will now contain exactly three cherries. The cherries will remain deep red, glossy, and attached to their stems, but the excess cherries will now need to be removed to meet the specified count. The rest of the composition, including the goblet, lemon peel, grapes, lemons, large yellow fruit, green fabric, and wooden table, will remain unchanged. The overall balance and aesthetic of the scene will be preserved.

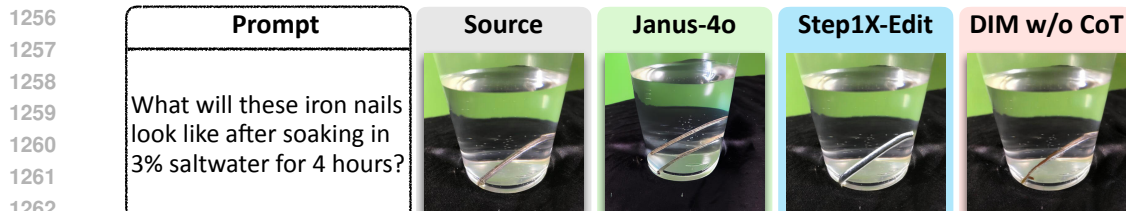
DIM-4.6B-Edit



1240
1241

Figure 12: The edits of **Janus-4o**, **Step1X-Edit**, **DIM w/o CoT**, and **DIM-4.6B-Edit** when the user instruction requires causal reasoning. DIM CoT is capable of *advanced causal editing* under this case.

1242
1243
1244
1245
1246
1247
1248
1249
1250
1251
1252
1253
1254
1255



1263 **Is there any chemical reaction that will
1264 change the appearance of the iron nail?**
1265

DIM CoT: Advanced Temporal Editing

1. Edit Instruction: What will these iron nails look like after soaking in 3% saltwater for 4 hours?
 2. Global Layout Perception: The image shows a transparent plastic cup filled with clear water. Inside the cup, there is a single iron nail submerged in the water. The cup is placed on a black fabric background, and the green wall is visible in the background.
 3. Local Object Perception:
 - **Iron Nail**: The nail is metallic, straight, and has a shiny silver-gray surface. It appears smooth and uncorroded.
 - **Water**: The water is clear and transparent, filling most of the cup.
 - **Cup**: The cup is made of clear plastic, cylindrical in shape, and allows visibility of its contents.
 - **Background**: The black fabric is textured and contrasts with the green wall behind it.
 4. Edit Area Localization: The iron nail inside the cup will change in appearance due to the soaking process.
 5. Edited Image Imagination: After soaking in 3% saltwater for 4 hours, the iron nail will likely show signs of corrosion. Its surface will appear duller, with possible reddish-brown rust spots forming, especially near the submerged portion. The water may also appear slightly cloudy due to the release of iron particles or rust. The cup and background will remain unchanged."

DIM-4.6B-Edit

1280 Figure 13: The edits of **Janus-4o**, **Step1X-Edit**, **DIM w/o CoT**, and **DIM-4.6B-Edit** when
1281 the user instruction requires temporal reasoning. DIM CoT is capable of *advanced temporal editing*
1282 under this case.
1283
1284
1285
1286
1287
1288
1289
1290
1291
1292
1293
1294
1295

1296

1297

1298

1299

1300

1301

1302

1303

1304

1305

1306

1307

1308

1309

1310

1311

1312

1313

1314

1315

1316

1317

1318

1319

1320

1321

1322

1323

1324

1325

1326

1327

1328

1329

1330

1331

1332

1333

1334

1335

1336

1337

1338

1339

1340

1341

1342

1343

1344

1345

1346

1347

1348

1349

B.3 VISUALIZATION OF FAILURE CASES

We are also open to discuss the limitations of our work, and provide three failure types with six specific cases in Figure 14, 15, and 16 to intuitively show the boundaries of our DIM-4.6B-Edit.

Large-scale All-in-One Editing. In Figure 14, the instructions involve simultaneous multi-step edits, a task that remains essentially challenging for almost all editing models, and one where DIM-Edit also encounters difficulties.

- For the first case, Janus-4o and Step1X-Edit completely fail to follow the physical laws dictating that the wooden tower should collapse. Our DIM-4.6B-Edit successfully imitates a scene of imminent collapse; however, it fails to preserve the exact appearance of the individual wooden blocks, as too many objects are involved in the manipulation.
- For the second case, Janus-4o and Step1X-Edit fail to change the view at all. While our DIM-4.6B-Edit completes the primary editing task, some fine-grained details are distorted (e.g., the window of the shoreside house is missing).

Text and Logic Editing. In Figure 15, where instructions involve complex text rendering and logical editing, DIM-4.6B-Edit struggles due to a combination of data scarcity and inherent VAE compression issues.

- For the first case, the use of SANA1.5’s VAE with a 32x downsampling rate makes complex text rendering particularly challenging, a difficulty exacerbated by the lack of targeted training data. In contrast, Step1X-Edit employs an 8x downsampling VAE and is trained on proprietary, text-specific in-house data, allowing it to perform relatively well. We regard this as a necessary trade-off between efficiency and rendering quality: as shown in Table 10, DIM-4.6B-Edit requires only 6 seconds to complete an edit with a 200+ word CoT, whereas Step1X-Edit takes 28 seconds with a short raw prompt.
- For the second case, all editing models fail. This is fundamentally because none of the models, including DIM-4.6B-Edit, are specifically trained on geometric data. The underlying painter struggles to even draw these shapes, let alone edit them. We believe crafting such datasets remains a valuable and under-explored topic for future research.

Reference-free Editing (in Pixel Space). In Figure 16, the reference image does not provide a strong pixel constraint for the target image. Consequently, this task resembles multimodal generation rather than strict editing. All models fail here because existing editing architectures typically enforce strong pixel alignment with the source image.

- For the first case, which requests a view of the Golden Gate Bridge, Janus-4o and Step1X-Edit are completely ineffective. DIM-4.6B-Edit struggles to break free from the structural constraints of the reference image, resulting in a “scratches” and distorted view that fails to meet the objective.
- For the second case, where the task involves a re-imagination of the source scene, Janus-4o produces a black-and-white edit, and Step1X-Edit fails completely. DIM-4.6B-Edit generates the most plausible result, successfully covering the scene with white snow. However, because the transformation fundamentally alters the source structure, specific details such as the castle are inevitably distorted.

In summary, the majority of failure cases arise when the task necessitates either generating an image that diverges drastically from the source or rendering complex text and geometric shapes. Even in these challenging scenarios, DIM-4.6B-Edit demonstrates superior instruction-following capabilities compared to baseline models. These limitations highlight persistent challenges within the current landscape of open-source editing models. We suggest that future research directions, such as intelligent routing that dynamically selects between T2I generation and editing pipelines based on instruction intent, offer promising avenues for resolving these issues, though significant progress is still required in the field.

1350

1351

1352

1353

1354

1355

1356

1357

1358

1359

1360

1361

1362

1363

1364

1365

1366

1367

1368

1369

1370

1371

1372

1373

1374

1375

1376

1377

1378

1379

1380

1381

1382

1383

1384

1385

1386

1387

1388

1389

Failure Type: Large-scale All-in-One Editing				
Prompt	Source	Janus-4o	Step1X-Edit	DIM-4.6B-Edit
Predict what happens when one wooden block is removed from the third layer (counting from bottom) of this tower.				
Failure Case: Spatial Reasoning + Massive Object Manipulation				
Prompt	Source	Janus-4o	Step1X-Edit	DIM-4.6B-Edit
Generate the view from a boat position 3 meters forward showing the building on the right bank in oil painting style.				
Failure Case: Viewpoint Change + Style Transfer				

Figure 14: The edits of **Janus-4o**, **Step1X-Edit**, and **DIM-4.6B-Edit** for the failure type *large-scale all-in-one editing*.

1375

1376

1377

1378

1379

1380

1381

1382

1383

1384

1385

1386

1387

1388

1389

1390

1391

1392

1393

1394

1395

1396

1397

1398

1399

1400

1401

1402

1403

Failure Type: Text & Logic Editing				
Prompt	Source	Janus-4o	Step1X-Edit	DIM-4.6B-Edit
Change the text 'ESTATE TACHEN' to 'Timeless Fashion'				
Failure Case: Complex Text Rendering				
Prompt	Source	Janus-4o	Step1X-Edit	DIM-4.6B-Edit
Find x. Please annotate your answer directly on the image.				
Failure Case: Geometry Understanding				

Figure 15: The edits of **Janus-4o**, **Step1X-Edit**, and **DIM-4.6B-Edit** for the failure type *text and logic editing*.

1404
1405
1406
1407
1408
1409
1410
1411
1412
1413
1414
1415
1416
1417
1418
1419
1420
1421

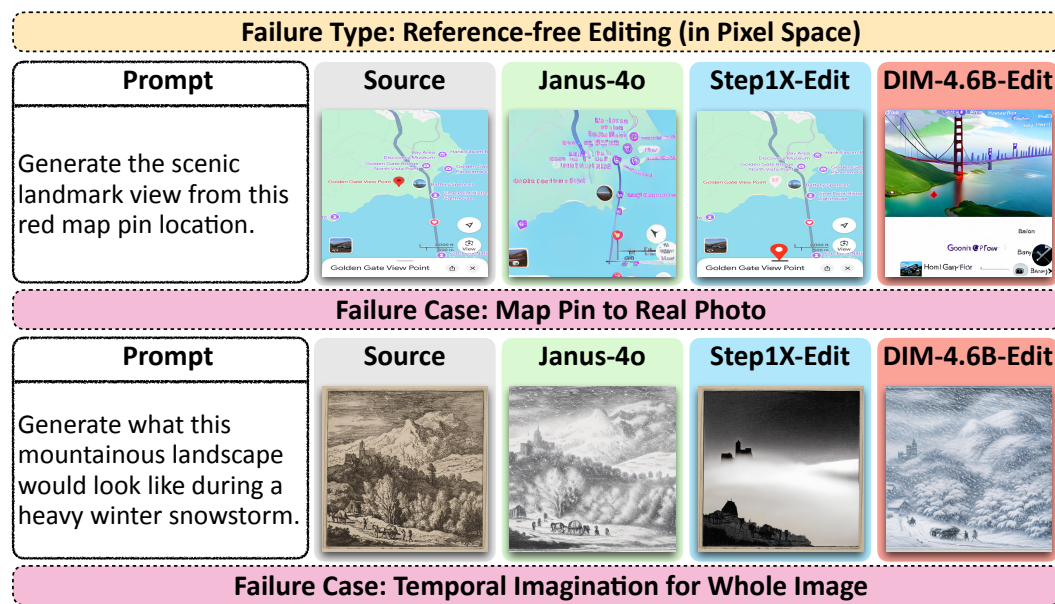


Figure 16: The edits of **Janus-4o**, **Step1X-Edit**, and **DIM-4.6B-Edit** for the failure type *reference-free editing (in pixel space)*.

1443
1444
1445
1446
1447
1448
1449
1450
1451
1452
1453
1454
1455
1456
1457

1458 **C DIM-EDIT DATA COLLECTION PIPELINE**
 1459

1460 As stated in Section 3.1.2, we collect raw edit data from four publicly available datasets:
 1461

- 1462 • **UltraEdit** (Zhao et al., 2024). In addition to the prompt quality evaluation and optimization in the
 1463 DIM-Edit creation pipeline (Figure 2), which aligns textual prompts with actual editing behaviors,
 1464 we employ three *image-to-image* metrics on the UltraEdit dataset to improve visual consistency
 1465 and stabilize training: (i) CLIP image similarity, (ii) DINOv2 similarity, and (iii) SSIM. These
 1466 metrics are used to select edit pairs that maintain consistent visual appearances. We retain only
 1467 those edit pairs that satisfy the following conditions: (i) the CLIP similarity between the source
 1468 and edited images is greater than 0.9; (ii) the DINOv2 similarity is greater than 0.9; (iii) the
 1469 SSIM score is greater than 0.8; and (iv) the prompt does not contain “rainbow”, since many edit
 1470 pairs meeting (i)–(iii) are associated with low-quality “rainbow” edits. After filtering, we obtain
 1471 roughly 160K edit pairs.
 1472
- 1473 • **MagicBrush** (Zhang et al., 2023). We include only 8K images from the training set to avoid
 potential information leakage during evaluation.
 1474
- 1475 • **SEED-Data-Edit-Part3** (Ge et al., 2024). Since the “remove” operation is absent in UltraEdit, we
 1476 additionally select 19K edit pairs from SEED-Data-Edit-Part3 by filtering prompts that explicitly
 contain “remove.”
 1477
- 1478 • **ShareGPT-4o-Image** (Chen et al., 2025b). We include only its 46K image-to-image subset.
 1479

1480 By combining these collected datasets, we obtain a total of 233K raw edit pairs for the proposed
 1481 DIM-Edit.
 1482

1483 **D DIM-EDIT QUALITY ASSESSMENT**
 1484

1485 We further assess the quality of the CoTs in DIM-Edit through MLLM-powered validation. Specifically,
 1486 due to API quota limitations, we randomly sample 30K edit pairs from DIM-Edit and use
 1487 GPT-4.1 to evaluate the quality of the GPT-4o-annotated CoTs, categorizing them into four levels:
 1488

- 1489 • **Low**: The optimized edit instruction does not re-
 1490 flect the change between the source and edited im-
 1491 ages at all.
 1492
- 1493 • **Medium**: The optimized edit instruction captures
 1494 the major change between the source and edited
 1495 images, but the chain-of-thought contains some
 1496 factual errors.
 1497
- 1498 • **High**: The optimized edit instruction captures the
 1499 major change between the source and edited im-
 1500 ages, and the chain-of-thought contains only mi-
 1501 nor factual errors.
 1502
- 1503 • **Ultra-High**: The optimized edit instruction accu-
 1504 rately captures all changes between the source and
 1505 edited images, and the chain-of-thought contains
 1506 no factual errors.
 1507

1507 The percentage distribution of each quality level is
 1508 shown in Figure 17. Notably, no data is categorized
 1509 as “Low”, while the majority falls under the “Ultra-
 1510 High” level, demonstrating the strong overall quality
 1511 of DIM-Edit.

1512 We further conducted a human verification study. Specifically, we randomly sampled 25 instances
 1513 from each of the data sources listed in Appendix C, resulting in a comprehensive evaluation set of
 1514 100 samples. Three human annotators were then recruited to assess the quality of the CoTs from
 1515 two distinct perspectives:

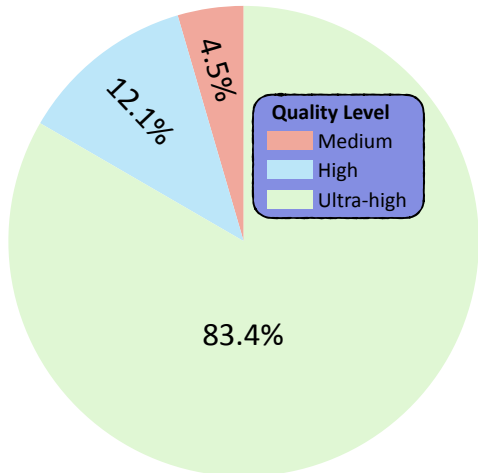


Figure 17: The percentage distribution of each quality level in DIM-Edit judged by GPT-4.1.

1512
1513
1514
1515
1516
1517
1518
1519
1520
1521

DIM-Edit CoT User Study

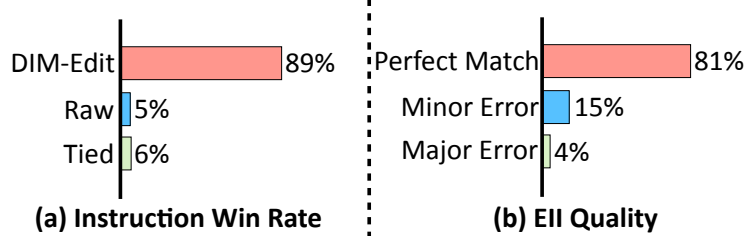


Figure 18: (a) The win rate of the optimized DIM-Edit instruction and the raw instruction. (b) The quality of the Edited Image Imagination (EII).

Evaluation of Optimized Instructions (Start of CoT). We presented annotators with both the raw instructions and the optimized instructions from DIM-Edit, alongside the corresponding source-edit image pairs. Annotators were tasked with selecting the instruction that best reflected the actual editing operations. A "Tied" option was included for cases where neither instruction was sufficiently accurate. The metric reported is the average win rate for each instruction type.

Evaluation of Edited Image Imagination (End of CoT). We asked annotators to assess the alignment between the Edited Image Imagination (EII) and the actual edited image. The quality was categorized into three levels: (i) Perfect Match, (ii) Minor Errors, and (iii) Major Errors. The metric reported is the percentage distribution across these error levels.

This efficient evaluation protocol enables a rapid yet robust assessment of the overall CoT quality within DIM-Edit. The results for both the instruction optimization (Win Rate) and the Edited Image Imagination (Error Distribution) are summarized in Figure 18, in which we have the following analysis:

- *Consistency with MLLM Assessment.* These results align closely with the MLLM-based quality assessment presented in Appendix D, where over 80% of DIM-Edit CoTs were judged clearer than the raw instructions, with no factual errors detected. Even in "Tied" cases where the optimization was not deemed strictly superior, the semantics of the raw instruction were fully preserved, ensuring that the optimization process introduces no regression.
- *Analysis of Minor Errors.* We observed that minor errors typically relate to subtle environmental inconsistencies, such as slight shifts in brightness (e.g., "the image should be a bit lighter"). These artifacts usually stem from the VAE's inability to perfectly reconstruct raw images in AI-generated pairs (e.g., from UltraEdit), leading to a slight loss of high-frequency features. As these discrepancies are barely perceptible to the human eye, they have a negligible impact on overall training efficiency.
- *Analysis of Major Errors.* Instances classified as having major errors generally correspond to extremely challenging scenarios where the edits are minute (e.g., the removed object occupies less than 2% of the pixels). These cases are difficult even for human annotators and advanced MLLMs like GPT-4o. Given their extreme rarity, these outliers do not adversely affect the stability of the training procedure.

Overall, the CoTs produced by our DIM-Edit pipeline maintain high quality and serve as effective design blueprints. This high data quality directly translates to better editing capabilities, as evidenced by the superior performance of the DIM-4.6B-Edit model trained on this dataset.

1559
1560
1561
1562
1563
1564
1565

1566 E DIM-T2I ANALYSIS DIMENSIONS
15671568 Figure 19 and 20 illustrate the 21 analysis dimensions and their corresponding prompts used in the
1569 DIM-T2I annotation process. **The 21 dimensions were derived from a thorough literature review and**
1570 **an empirical analysis of existing understanding datasets and benchmarks. They are listed as follows:**1571 MME (Fu et al., 2025), MMMU (Yue et al., 2024), MMMU-Pro (Yue et al., 2025),
1572 MMLU (Hendrycks et al., 2020), MMStar (Chen et al., 2024b), MMT-Bench (Ying et al.,
1573 2024), MM-Vet (Yu et al., 2023), MM-Vet V2 (Yu et al., 2024), LLaVA-Bench-Wild (Liu et al.,
1574 2023a), LLaVA-Bench-Wilder (Li et al., 2024a), WildVision (Lu et al., 2024), COCO (Lin et al.,
1575 2014), VQAv2 (Goyal et al., 2017), OK-VQA (Marino et al., 2019), TextCaps (Sidorov et al.,
1576 2020), TextVQA (Singh et al., 2019), AI2D (Kembhavi et al., 2016), ChartQA (Masry et al.,
1577 2022), DocVQA (Mathew et al., 2021), MathVista (Lu et al., 2023), MIA-Bench (Qian et al.,
1578 2024), MegaBench (Chen et al., 2024a), RWQA (xAI, 2024), OCRBench (Liu et al., 2023b),
1579 GSM8K (Cobbe et al., 2021), GPQA (Rein et al., 2024), IFEval (Zhou et al., 2023).1580 We believe that the aspects emphasized in widely recognized understanding datasets and benchmarks
1581 effectively capture the most frequent interactions between humans and objects in the real
1582 world. This makes them an ideal foundation for learning text-to-image generation tasks involving
1583 long and complex instructions. By constructing prompts that span these diverse fields, DIM-4.6B-
1584 T2I not only masters long-form instruction processing but also acquires the broad world knowledge
1585 necessary to facilitate sophisticated CoT comprehension and precise editing, thereby achieving high
1586 GenEval scores and low FID on MJHQ-30K.1587
1588 F THE USE OF LARGE LANGUAGE MODELS
15891590 This paper uses OpenAI ChatGPT solely for polishing the writing. The authors provided raw text
1591 to ChatGPT to correct grammatical errors and refine the statements into a more formal academic
1592 style. All polished text was manually reviewed and verified by the authors, who affirm that the
1593 paper contains no fabricated content. No statistical data were provided to ChatGPT. All numerical
1594 values in tables and figures were originally written by the authors.1595
1596
1597
1598
1599
1600
1601
1602
1603
1604
1605
1606
1607
1608
1609
1610
1611
1612
1613
1614
1615
1616
1617
1618
1619

1620

1621

1622

1623

1624

1625

1626

1627

1628

1629

1630

1631

1632

1633

1634

1635

1636

1637

1638

1639

1640

1641

1642

1643

1644

1645

1646

1647

1648

1649

1650

1651

1652

1653

1654

1655

1656

1657

1658

1659

1660

1661

1662

1663

1664

1665

1666

1667

1668

1669

1670

1671

1672

1673

Dimension	Prompt
System Message	Please describe images in details, including but not limited to the user pre-defined dimensions. Please make sure your description is visually grounded for user provided image, namely the user can find visual cues in image for your generated image caption. The user pre-defined dimensions are: [DIMENSIONS] Please don't generate your response for each dimension, e.g., **something**, just give an overall image caption including all the dimensions.
Character Name	If a character is shown in the image, you must describe his/her names. The character include but not limited to the characters shown in Movies, TV Shows, Anime, Comics, Literature, Games, Virtual Idols/Characters.
Scene Description	Provide an overview of the image, identifying key objects, people, and any interactions. Clearly classify and describe each object (e.g., people, animals, buildings, plants). Specify their attributes, such as size, color, material, and texture.
Actions and Interactions	Describe any actions taking place in the image. Who is performing them, and how are they interacting with other objects or people? If there are dynamic elements (e.g., movement), detail their state (e.g., running, jumping, flying, waving).
Context and Environment	Describe the setting of the image, including the location (indoor or outdoor), time of day, weather, and any background elements (e.g., sky, buildings, roads). How does the environment contribute to the overall scene? Does the setting enhance the mood or theme?
Emotion and Sentiment	If people are present, describe their emotional states based on body language, facial expressions, and other visual cues. What mood or tone does the image convey (e.g., happiness, sadness, tension, peace)? How do these emotions connect to the scene?
Relationships and Spatial Arrangement	Explain how objects, people, and other elements are positioned in relation to one another (e.g., "next to," "above," "to the right of"). Consider foreground, background, and overall spatial composition. How does the positioning influence the overall visual balance or narrative?
Color and Texture	Describe the color palette of the image (e.g., colors of objects, background), and note any texture details (e.g., smooth, rough, soft). How do these color and texture choices contribute to the atmosphere or style of the image?
Symbolism or Abstract Interpretation	If relevant, interpret any symbolic or abstract elements within the image. What deeper meanings or metaphors can be inferred from the visual elements? How do these symbols tie into the image's broader themes or message?
Lighting and Shadows	Observe the lighting conditions in the image (e.g., sunlight, artificial light) and how shadows or reflections influence the objects' appearance. Note the intensity of the light and any patterns created by it. How do these lighting effects contribute to the mood or focal points of the image?
Details and Fine Elements	Focus on smaller, intricate details in the image (e.g., wrinkles in clothing, textures on surfaces, distinct features). These elements may carry significant meaning or help provide a more vivid, precise description.

Figure 19: The 21 analysis dimensions and corresponding prompts for DIM-T2I.

1674

1675

1676

1677

1678

1679

1680

1681

1682

1683

1684

1685

1686

1687

1688

1689

1690

1691

1692

1693

1694

1695

1696

1697

1698

1699

1700

1701

1702

1703

1704

1705

1706

1707

1708

1709

1710

1711

1712

1713

1714

1715

1716

1717

1718

1719

1720

1721

1722

1723

1724

1725

1726

1727

Dimension	Prompt
Perspective and Composition	Describe the viewpoint of the image (e.g., aerial, eye-level, side view) and its composition (e.g., symmetry, balance, focal point). How does the choice of perspective and composition affect the viewer's perception or interpretation of the scene?
Time and Season	If possible, infer the time of day or season based on visual cues (e.g., light quality, weather, clothing style). For example, a winter snow scene, a summer beach setting, or an autumn forest could suggest the specific season.
Target Audience	Consider if there's a specific target audience for the analysis. For instance, an analysis for an art historian might use more technical terms, while one for a general audience may keep the description simpler. Does the complexity of the image suggest it's meant for a particular demographic or purpose?
OCR	If text appears in the image, you must describe the text in its original language and provide an English translation in parentheses. For example: 书本 (book). Additionally, explain the meaning of the text within its context.
Person Description	If there are people in the image, describe their physical features (e.g. age, gender, hairstyle, clothing, etc.), their movements and expressions, and their relationship to the surrounding environment. If there is a single person, use 'he' or 'she' for reference instead of 'they'.
Mathematics	Analyze the image and describe the mathematical concepts it represents. Include specific details like geometric shapes, equations, numeric values, or relationships between elements. If the image includes a graph, describe its axes, scales, and key points. If applicable, explain how mathematical operations are visualized.
Information Extraction	Examine the image and extract textual and contextual information. If the image contains a document, transcribe its content accurately. For GUI or structured data, describe its layout, labels, and functionality. Summarize the core message or purpose of the content.
Planning	Identify the sequence or logical arrangement in the image. If it depicts a process, explain the steps and their correct order. For puzzles or games, provide the rules and possible solutions.
Science	Explain the scientific content or phenomenon depicted in the image. Provide details on experiments, natural phenomena, or theoretical concepts, including relevant terminology.
Perception	Provide a detailed perception-based description of the image. Identify objects, their attributes (color, shape, size), and spatial relationships. For specific tasks like facial analysis or pose estimation, include characteristics like expressions, poses, or physical traits.
Metrics	Evaluate the image based on predefined metrics. Assess its quality, authenticity, and adherence to caption content. For paper review or comparative tasks, provide constructive feedback or preference reasoning.

Figure 20: The 21 analysis dimensions and corresponding prompts for DIM-T2I. (Continue)